An analysis of soil respiration across northern hemisphere temperate ecosystems [☆]

K.A. HIBBARD[1,2,*], B.E. LAW[1], M. REICHSTEIN[1] and J. SULZMAN[1]

[1]*Oregon State University, Forest Science, 304 Richardson Hall, Corvallis, OR 97331, USA;*
[2]*National Center for Atmospheric Research, Box 3000, Boulder, Co 80303, USA; *Author for
correspondence (e-mail: kathy.hibbard@oregonstate.edu)*

Key words: Arrhenius model, Biotic controls, Ecosystem modelling, Environmental controls, Labile carbon, Soil respiration

Abstract. Over two-thirds of terrestrial carbon is stored belowground and a significant amount of atmospheric CO_2 is respired by roots and microbes in soils. For this analysis, soil respiration (Rs) data were assembled from 31 AmeriFlux and CarboEurope sites representing deciduous broadleaf, evergreen needleleaf, grasslands, mixed deciduous/evergreen and woodland/savanna ecosystem types.Lowest to highest rates of soil respiration averaged over the growing season were grassland and woodland/savanna < deciduous broadleaf forests < evergreen needleleaf, mixed deciduous/ evergreen forests with growing season soil respiration significantly different between forested and non-forested biomes ($p < 0.001$). Timing of peak respiration rates during the growing season varied from March/April in grasslands to July–September for all other biomes. Biomes with overall strongest relationship between soil respiration and soil temperature were from the deciduous and mixed forests ($R^2 \geq 0.65$). Maximum soil respiration was weakly related to maximum fine root biomass ($R^2 = 0.28$) and positively related to the previous years' annual litterfall ($R^2 = 0.46$). Published rates of annual soil respiration were linearly related to LAI and fine root carbon ($R^2 = 0.48, 0.47$), as well as net primary production (NPP) ($R^2 = 0.44$). At 10 sites, maximum growing season Rs was weakly correlated with annual GPP estimated from eddy covariance towersites ($R^2 = 0.29; p < 0.05$), and annual soil respiration and total growing season Rs were not correlated with annual GPP ($p > 0.1$). Yet, previous studies indicate correlations on shorter time scales within site (e.g., weekly, monthly). Estimates of annual GPP from the Biome-BGC model were strongly correlated with observed annual estimates of soil respiration for six sites ($R^2 = 0.84$; $p < 0.01$). Correlations from observations of Rs with NPP, LAI, fine root biomass and litterfall relate above and belowground inputs to labile pools that are available for decomposition. Our results suggest that simple empirical relationships with temperature and/or moisture that may be robust at individual sites may not be adequate to characterize soil CO_2 effluxes across space and time, agreeing with other multi-site studies. Information is needed on the timing and phenological controls of substrate availability (e.g., fine roots, LAI) and inputs (e.g., root turnover, litterfall) to improve our ability to accurately quantify the relationships between soil CO_2 effluxes and carbon substrate storage.

Abbreviations: ET – evapotranspiration (g H_2O m^{-2}) derived from eddy covariance towers; GPP – gross primary production (gC m^{-2}, NPP + Ra); LAI–leaf area index (m^2 leaf m^{-2} ground, projected); NEE – net ecosystem exchange (gC m^{-2}) derived from eddy covariance towers; NEP –

net ecosystem production (gC m^{-2}) (NEP = GPP − (Ra + Rh)); NPP – net primary production (gC m^{-2}) (wood + foliage + roots); Ra – autotrophic (plant) respiration; Re – Rs + heterotrophic respiration from litter + woody debris; Rh – heterotrophic (microbial plus animal) respiration; Rs – soil respiration (Ra + Rh)

Introduction

The global carbon cycle is intrinsically tied to climate, hydrology, nutrient cycles and the production of biomass through photosynthesis on land and in the oceans. Estimates of global soil CO_2 emissions are highly uncertain and exceed annual fossil fuel emissions by 11–20 times, ranging from 75 to 120 Gt C CO_2 yr^{-1} (Raich and Potter 1995; Schimel et al. 1996). In recent decades, atmospheric CO_2 concentrations have consistently increased and it is expected that the rate of increased atmospheric CO_2 growth will double over the next century (IPCC 2001). The interannual variability in net ecosystem exchange with the atmosphere has been largely attributable to terrestrial ecosystems. Net ecosystem production (NEP) is the difference between net primary production by plants (NPP) and respiratory losses by heterotrophs (Rh). Typically, decomposers respire about 99% of autotrophic inputs (Schlesinger 1990), however, the net balance between production and heterotrophic respiration can be up to 10% in absolute value of gross primary production (GPP), and is often negative when respiratory fluxes exceed those of production.

Over two-thirds of terrestrial carbon is stored belowground and a significant amount of the atmospheric CO_2 assimilated by plants is respired by roots and microbes in terrestrial soils. Soil respiration is therefore a key process that underlies our understanding of the terrestrial carbon cycle. Soil respiration (Rs) consists of root (autotrophic) respiration and microbial (heterotrophic) respiration of soil carbon. Several factors contribute to soil CO_2 efflux including photosynthetic supply to roots, substrate quality and availability, temperature and moisture (Figure 1). Despite this complexity, a number of studies, particularly on large spatial scales, have used very simple, often purely climate-driven models to predict soil respiration (Raich and Schlesinger 1992; Raich et al. 2002). At the plot scale, several studies have analyzed the relative contribution of environmental controls including soil temperature and moisture, substrate availability and quality, soil C decomposition and microbial growth dynamics, soil hydraulic properties, as well as root maintenance and growth requirements on rates of respired CO_2 from soils (cf., Borken et al. 2002; Davidson et al. 2002; Reichstein et al. 2002a; Sanderman et al. 2003; Gu et al. 2004). Many recent synthesis studies have utilized Arrhenius equations (e.g., developed from Lloyd and Taylor 1994) to investigate soil respiration dependencies on environmental factors such as soil temperature, soil moisture and biotic constraints including LAI (e.g., Janssens et al. 2001; Reichstein et al. 2003; Sanderman et al. 2003). Other modeling activities have utilized ecosystem models to test hypotheses regarding carbon allocation and belowground
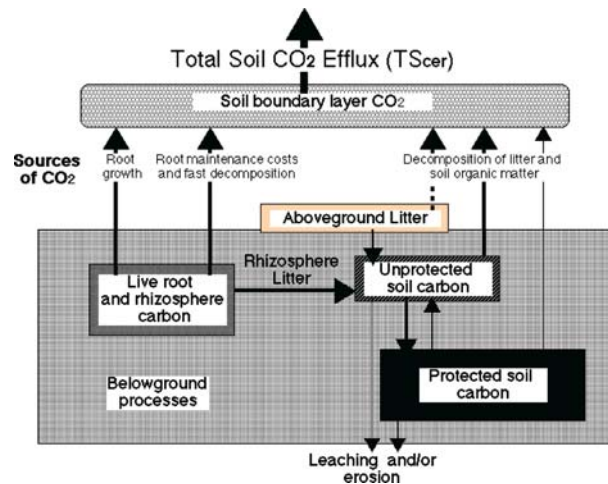
Figure 1. Biological processes leading to the CO_2 fluxes within the soil and surface boundary layer (Figure courtesy of P. Hansen).

processes on carbon stocks and fluxes (Kramer et al. 2002; Thornton et al. 2002; Churkina et al. 2003; Law et al. 2003).

We present an integrated measured and modeled process-oriented analysis utilizing soil respiration data that were assembled from 31 AmeriFlux and CarboEurope sites representing deciduous broadleaf, evergreen needleleaf, grasslands, mixed deciduous/evergreen and woodland/savanna ecosystems. The purpose of this paper is to analyze measured rates of soil respiration based on (1) synthesis to a common time step and (2) an ecosystem model, Biome-BGC (Thornton 1999). In the first analysis, we discuss the relationship of the data to abiotic (soil temperature and moisture) and biotic (LAI, fine root carbon) factors that contribute to average daily, seasonal and annual variability of fluxes within sites and across biomes. In the second analyses, we evaluate seasonal dynamics and model performance relative to observed carbon stocks and the components of respired fluxes for five sites representing evergreen needleleaf, deciduous broadleaf and woodland/savanna in Europe and the US. We conclude by evaluating the variability in observed and modeled respiration rates and their relationship to fast residence carbon pools (e.g., labile) and to changes in long term carbon storage.

Methods

Description of sites

This study includes sites from deciduous broadleaf (DBF) and evergreen needleleaf (ENF) forests, a mixed deciduous/evergreen forest (MXD), grasslands

(GRS), and woodland/savannas (WSV). The geographic range of these northern hemispheric sites is from 33° to 51°N latitude and 124°W to 13°E in longitude (Table 1). The climatic zones include temperate continental and temperate oceanic, subalpine and Mediterranean. The study sites range in age from 3 to 300 years and include managed and unmanaged forests, grazed and ungrazed grasslands and unmanaged woodland/savannas. General site characteristics including site labels are listed in Table 1.

Estimates of annual net primary production (NPP) were available from seven forested and one woodland/savanna site and ranged from 313 to 922 gC m^{-2} yr^{-1}. Annual estimates of ecosystem respiration (Re) were available from 13 sites ranging from 240 gC m^{-2} yr^{-1} in Sisters Juniper WSV to 1680 gC m^{-2} yr^{-1} at the Bray ENF site. Ecosystem respiration is the sum of autotrophic respiration (live foliage, wood, roots), soil autotrophic and heterotrophic respiration, and respiration associated with heterotrophic decomposition of litter and woody debris. Published, annual estimates of soil respiration (Rs) based on interpolated chamber measurements were available for 13 sites and ranged from 438 to 1805 gC m^{-2} yr^{-1} in the Vielsalm and HJ Andrews ENF forests. Annual estimates based on chamber measurements from GRS and WSV biomes were not available. All sites contributed estimates of LAI, ranging from 0.77 at the semiarid Sisters Juniper site in Oregon to 7.6 m^2 m^{-2} at the German ENF site, Tharandt. Estimates of soil C and fine roots at variable depths were available from 13 and 10 sites, respectively. Site carbon pools and fluxes are detailed in Table 2.

Measurements

Several sites contributed multiple datasets representing various components of their ecosystems (see Table 1). Metolius contributed three datasets; one was from a chronosequence of 12 ponderosa pine sites (MEC) using manual chamber measurements (Campbell and Law this issue), and the other two were from automated chamber measurements made at the young and old pine flux-tower sites (MEO, MEY) (Irvine and Law 2002). To maintain a consistent analysis with regard to stand age and structure from evergreen needleleaf forests represented in this study, only data from the young and mature stands (22–52, 40–170 and 56–106 yr) at the Oregon sites (CHD, HJA, MEC), respectively, were included. See Campbell and Law (this issue) for details on soil fluxes of all four stand-age classes. The Oregon Sisters juniper dataset (JUN) was previously unpublished (Law, unpublished data). The Ione grassland site (ION) in California contributed manual chamber measurements (ION) and modeled (IOM) soil respiration derived from tower flux data (Xu and Baldocchi 2004). The Great Basin in Utah submitted data from cheatgrass and western wheatgrass (GBC, GBR) grasslands as well as sagebrush, and juniper (GBS, GBJ) woodland/savannas, Sky Oaks submitted data from old (SKO) and young (SKY) savannas in California, the de Inslag site in Belgium

Table 1. Site characteristics, including mean annual temperature (MAT), mean annual precipitation (MAP), stand age at end of submitted Rs, stand history and years of Rs in this analysis.

Site	Location	Elevation (m)	Climate[a]	MAT(° C)	MAP(mm)	StandAge	History[b]	Rs submitted
Evergreen needleleaf Forest (ENF)								
BEP	51.31N 4.31E	16	TC	10	770	67	P/1929[c]	2001
BIL	44.72N 0.77E	60	M	13.5	916	3		2000–2002
BRY	44.72N 0.77E	60	M	13.5	916	25	P/, S/1999	2000–2002
CHD	45.1N 123.9W	122–321	TO	10.5	2800			2001–2002
DUK	35.97N 79.1W	120–163	T	15.5	1147	17	CC, B, P/1983	1998–2001
HJA	44.25N 122.19W	712–846	T	8.3	2100			2001–2002
HOW	45.2N 68.7W	60	TC	5.69	1040	90		1997–2001
HRM	44.72N 0.77E	60	M	13.5	916			2000–2002
MEO	44.5W 121.62N	915–1141	T	8.5	530	50–250		1996, 1997, 1999–2001
MEY	44.5W 121.57N	1188	T	7.25	466	15	CC	1999–2001
MEC	44.43N 121.63W	887–1232	T	8	550	9–300		2001–2002
NIW	40.0N 105.6W	3050	TS	4	800	95		1999–2001
THA	50.96N 13.75E	380	TC	7.6	820	113		2000–2002
TML	44.72N 0.77E	60	M	13.5	916			2000–2002
VLD	50.3N 6.0E	450	TO	7	1000	75	P/1935-1960[c]	1997–1998
WDN	50.09N 11.52E	765–780	TO	6.0	1019	112	P	1999
Mixed deciduous/evergreen forest (MXD)								
UMB	45.56N 84.71W	234	TN	6.2	750	90		1998–2000
HAR	42.54N 72.17W	180–490	T	7.85	1066	60–90	S	1995–2001
WCR	45.8N 90.12W	520	CC	4.8	818	66	CC	1998–1999
Deciduous broadleaf forest (DBF)								
BEQ	51.31N 4.52E	16	TC	10	1168	67	P/1936[c]	2001
HES	48.67N 7.08E	300	M	9.7	950	31–36	CC, S/1999	1996–2000
VLB	50.3N 6.0E	450	TO	7	1000	75	P/ 1908[3]	1997–1998
Woodland/savanna (WSV)								
GBS	40.3N 112.47W	1650	TC	8.8	299			2001–2002
GBJ	40.28N 112.47W	1650	TC	8.8	299			2001–2002

33

Table 1. Continued

Site	Location	Elevation (m)	Climate[a]	MAT(° C)	MAP(mm)	StandAge	History[b]	Rs submitted
JUN	44.27N 121.38 W	945	T					1997, 2002
SKO	33.38N 116.62W	1385	M	12.2		78		2001
SKY	33.38N 116.62W	1421	M	12.2			B	1999–2001
TNZ	38.43N 120.97W	177	M	16.3	558.7	4	G	2001–2002
Grassland (GRS)								
GBC	40.28N 112.47W	1650	TC	8.8	299			2001–2002
GBR	40.28N 112.47W	1650	TC	8.8	299			2001–2002
ION	38.4N 120.95W	129	M	21.4	611		G	2001
IOM	38.4N 120.95W	129	M	21.4	611		G	2000–2001

Missing values indicate there were no data available.

[a] Climate: M, mediterranean; T, temperate; TC, temperate, continental; TS, temperate, subalpine; TO, temperate, oceanic; TN, temperate, northern; CC, cool, continental.

[b] CC, clearcut; B, burned; P, planted; S, storm; hurricanes G, grazing; BEP, Belgium de Inslag Pine; BIL, Bilos; BRY, Bray; CHD, Cascade Head; DUK, Duke; HJA, HJ Andrews; HOW, Howland; HRM, Herm; MEO, Metolius old; MEY, Metolius young; MEC, Metolius; NIW, Niwot; THA, Tharandt; TML, Temple; VLD, Vielsalm Douglas-fir; WDN, Weidenbrunnen; UMB, University Michigan Biological Station; BEQ, Belgium de Inslag Oak; HAR, Harvard; HES, Hesse; VLB, Vielsalm Beech; WCR, Willow Creek; GBS, Great Basin Sage; GBJ, Great Basin Juniper; JUN, Juniper (Oregon); SKO, Sky Oaks old; SKY, Sky Oaks young; TNZ, Tonzi; GBC, Great Basin Cheatgrass; GBR, Great Basin Crested Wheatgrass; ION, Ione Measured; IOM, Ione Modeled.

[c]http://carbodat.ei.jrc.it/data_arch_f.html.

Table 2. Site characteristics, including gross primary production (GPP), leaf area index LAI, net primary production (NPP), ecosystem respiration (Re), fine root carbon, litterfall, soil carbon, depth of soil carbon data, maximum soil respiration (Max Rs) and the range of published annual soil respiration.

Site	GPP[a]	LAI[b]	NPP[a]	R_e[a]	Fine roots[c]	Annual litterfall[a]	Soil C[c]	Soil C Depth(cm)	Max Rs[d] (this study)	Range of published annual Rs[a]	Reported year(s) of annual Rs[a]	Data citations
Evergreen needleleaf Forests (ENF)												
BEP	992	2.1		1033–1218	165	125	460	0–2	2.22			
BIL	727	1.9		996			5085	0–20	4.34			
BRY	2140	4.9		1527–1680					5.01			
CHD		9.6			595	198			5.82	1805	2001	Campbell and Law (this issue)
DUK	1487	5.2		1200		206–251			10.79			
HJA		7.4			936	130			12.46	1232	2001	Campbell and Law (this issue)
HOW	909	5.3				132–183			7.04	670–800	1996–1999	Davidson et al. (1998), Savage and Davidson (2001)
HRM		2.6							6.87			
MEO	1270	2.1	400–443	885	423, 197	49–216	5556	0–100	5.42	427–780	1996; 1999–2001	Law et al. (2001, 2003)
MEY	809	1.0, 1.5	308–317	835	317–500	44–88	6918	0–100	4.28	427–654	1999; 1999–2001	Law et al. (2001, 2003)
MEC		2.0	162–659		175	75			4.07	666	2001	Campbell and Law (this issue)
NIW	831	4.2			469		16,229; 3065	0–8	8.19			
THA	1680–1890	7.0–7.6		1071–1213			13,003	100	7.80			Wang et al. (2003)
TML		2.6							11.48			
VLD	1328	3.4		848–920					1.74	438	1997	Longdoz et al. (2000)
WDN	1319	7.4		1300	142		12,875	0–20	3.58	500–590	1999	Subke et al. (2003)
Mixed evergreen/deciduous forests (MXD)												
HAR	1122	4.0–5.5	565	950–1220		185–218	8800; 6700; 2000	0–60	9.56	640–860	1995; 1995–1999	Curtis et al. (2002)
UMB		3.7	540–632		470	118–135	1385	15	9.31	1132	1999	Curtis et al. (2002)

Table 2. Continued

Site	GPP[a]	LAI[b]	NPP[a]	R_e[a]	Fine roots[c]	Annual litterfall[a]	Soil C[c]	Soil C Depth(cm)	Max Rs[d] (this study)	Range of published annual Rs[a]	Reported year(s) of annual Rs	Data citations
WCR	902	5.4	264	769	245	135–147	10,700	0–30	7.62	810	1999	Martin and Bolstad (this issue)
Deciduous broadleaf forests (DBF)												
BEQ	992	3.4		1033–1218	133	198	1525		5.59			Longdoz et al. (2000)
HES	1226	7.3		793–1036	155	120–176	7400		4.11	509–713	1996–1998	Longdoz et al. (2000)
VLB	1328	5.2		848–920		158			4.63	867	1997	
Woodland/savannas (WSV)												
GBS		1.0							2.96			
GBJ		1.4							4.66			
JUN	734[e]	0.77/1.26		240	98	13–26	1344	0–10	1.51	181		Law (unpublished)
SKO	387	3.0		735–758					0.79			
SKY	798	1.1	798						0.92			
TNZ		0.6				58	4847	0–30	10.25	488	2002	Tang et al. (this issue); Z. Kayler pers comm.
Grasslands (GRS)												
GBC		0.9							5.72			
GBR		0.8							3.29			
ION		2.5							8.16			
IOM		2.0							7.00		2001–2002	Xu and Baldocchi (2004)

Site labels defined in Table 1.
[a] Units gC m^{-2} yr^{-1}.
[b] Units m^2 m^{-2}.
[c] Units gC m^{-2}.
[d] Units μmol m^{-2} s^{-1}.
[e] Model-derived estimate (Law, unpublished).

submitted data from ENF pine (BEP) and DBF oak (BEQ) forests; and the Vielsalm, Belgium site submitted DBF beech (VLB) and ENF Douglas-fir (VLD) datasets. Site characteristics and years of Rs data submitted to this analysis are in Table 1.

In all cases, Rs was measured at 6–15 locations per plot. Most sites submitted data using portable infrared gas analyzers (LI6200, LI6400, Licor, Inc., Lincoln, NE). Other portable analyzers (CIRAS I PP systems) were used at the BIL, BRY, DUK, HRM and TMP sites. Soil chambers were placed on pvc collars that were inserted in the ground at least 24 h before measurement. Chamber measurements from the Ione grassland were placed over grass, thus including dark respiration from live leaves; the autotrophic respiration from foliage was estimated to be 30% of the measured flux (Law et al. 2002; Sanderman et al. 2003; Xu and Baldocchi 2004). All other grassland measurements were made over the soil surface. Soil temperature was measured simultaneously with an attached temperature probe next to the soil collars (5–8 cm depth). At the Weidenbrunnen ENF site, soil CO_2 efflux was monitored by an automated open dynamic chamber system with five chambers sampling semi-continuously from 15 soil collars (Subke et al. 2003). Data collected with soda-lime methods were not included in this synthesis.

Many of the data contributed to this analysis were from flux-tower sites where the eddy covariance technique is used to estimate net ecosystem exchange (NEE). Automated micrometeorological measurements are made of CO_2 and water vapor exchange over vegetation at the sites, and ancillary data, such as soil properties, leaf area index (LAI), and NPP are collected. Many of the annual estimates of gross primary production (GPP), NEE, net ecosystem production (NEP), and LAI used in this analysis were previously reported in Law et al. (2002). Flux systems include three-axis sonic anemometers that measured wind speed and virtual temperature, infrared gas analyzers that measured concentrations of water vapor and CO_2, and software for real-time and post-processing analysis. For further details on flux calculations, see Falge et al. (2002) and Law et al. (2002).

Data processing

Measured Rs, soil temperature (Ts) and soil moisture (Sm) (when available) from 31 participating sites were synthesized to a common time-step representing average measured flux in a 24-h period (μmol m^{-2} s^{-1}). Average rates (μmol m^{-2} s^{-1}) for a day, month and year were calculated from datasets that included half-hourly, daily and sporadic measurements throughout a year. Site data were aggregated to five biome types: evergreen needleleaf (ENF), deciduous broadleaf (DBF), mixed deciduous/evergreen (MXD), grassland (GRS), and woodland/savanna (WSV). Summary statistics and correlation coefficients between Rs and Ts as well as Rs and Sm are listed in Appendix 1.

Three temporal scales were considered for site and biome analyses of the average fluxes for a day: mean flux for a given day of year, average flux measured over the course of a month, and growing seasonal average. The growing season average flux was determined as ± 60 days of maximum Rs flux, encompassing 4 months of data. All data within the 120 day window were averaged. Maximum growing season Rs was identified as the highest daily mean flux in a calendar year (μmol m^{-2} s^{-1}). Estimates of average fluxes in a growing season were calculated for individual years within ENF and DBF biomes. There were not enough data in GRS, WSV and MXD biomes for interannual estimates of soil respiration through the growing season, therefore the data were pooled for these growing season estimates.

Limitations
Individual site datasets that were complete enough to facilitate meaningful analyses at monthly and seasonal temporal scales included Belgium de Inslag, Brasschaat, Harvard, Hesse, Howland, modeled Ione, Metolius, Sisters Juniper, Niwot, Tharandt, Willow Creek and UMBS. Similarly, sites that contributed estimates of litterfall were from the Belgium de Inslag and Vielsalm forests, Cascade Head, Duke, HJ Andrews, Howland, Metolius, Harvard, UMBS, Willow Creek, Hesse and Sisters Juniper sites. Estimates of fine root biomass were available from Hesse, Metolius, Sisters Juniper, Niwot, Belgium de Inslag and UMBS. Direct measurements of Net Primary Production (NPP) were sparse, however, we utilized NPP as available from participating sites (Table 2).

Analyses

Simple regressions
Average fluxes in a day were compared to soil temperature and moisture across sites and biomes. Maximum rate of measured soil respiration and average growing season fluxes were empirically compared to LAI and fine root biomass when available. Annual estimates of soil respiration from the literature were evaluated relative to estimates of seasonal maximum LAI, fine root mass, annual GPP from eddy covariance data, and mean annual air temperature MAT (Table 2).

Temperature standardized respiration
The soil respiration data sets were analyzed for each site with a non-linear regression model that relates soil respiration to soil temperature (Lloyd and Taylor 1994):

$$R(T_{soil}) = R_{ref} \cdot e^{E_a \cdot \left(1_{ref}^{T} - t_0 - 1_{soil}^{T} - T_0\right)} \tag{1}$$

where T_{soil} (°C) is the soil temperature in the upper layer (usually at 5 cm depth), R_{ref} (μmol m^{-2} s^{-1}) is the expected respiration at the reference temperature (T_{ref}, °C), T_0 (°C) is the soil temperature at which respiration ceases,

and E_a (°C^{-1}) is a parameter that determines the temperature sensitivity of soil respiration, analogous to the activation energy in the common Arrhenius equation.

T_{ref} and T_0 were set to 15 and −46.02 °C (as in Lloyd and Taylor 1994). Results are largely independent of the choice of T_0 since E_a and T_0 parameters are strongly correlated in this model, while R_{ref} should not be considered a free parameter, but a parameter to standardize the respiration with respect to temperature. We estimated both a standardized Rs based on a single T_{ref} (R_{n15}) and developed the regression parameters E_a and R_{ref} estimated from the observed data for each month of the year and site via non-linear regression with the least-squares algorithm. The data were analyzed monthly to minimize confounding effects of abiotic and biotic factors on respiration. In contrast to the analyses performed by Reichstein et al. (2002b, 2003), soil water content was not considered directly and the temperature sensitivity was kept constant for each site/month combination. Thus the R_{ref} estimates reported here are not standardized to common water availability and can be affected by soil water deficit. This procedure was necessary to allow for a consistent analysis of data sets both with and without soil moisture data. Additionally, for comparisons with LAI, R_{ref} was filtered, or limited to sites with > 2 months of data, limiting this analysis to 12 sites. Our filtering technique would have limited comparisons of fine root data to five sites, therefore, all R_{ref} data were used in comparisons to fine roots.

Regressions for each site-month combination were only executed if more than six data points were available and regression results were considered acceptable if the relative standard error of the R_{ref} estimate was less than 50% and E_a stayed within an acceptable range relative to temperature (−10 to 500 °C), corresponding to Q_{10} values between ∼1 and 5. Average E_a response to temperature for the sites in this analysis was lowest at the dry Sky Oaks WSV and highest at Howland ENF. The activation energy parameter (E_a) is parameter in a non-linear function used to define the change in respiration relative to an expected rate constant (R_{ref}) over the inverse of temperature. As such, the relationship of E_a to temperature should not be interpreted to infer a direct response of respiration to temperature, but rather, an apparent sensitivity of the activation energy to site-specific conditions. For instance, E_a is sensitive to depth of measured soil temperature and the relationship of that temperature to the source of the respired flux. Even if measured soil temperature depths were standardized, the variable thermal diffusivities and soil physical properties confound the relationship between E_a and respiration. The standard error of the estimate was calculated according standard frequency assumptions of normality and independence of the residuals (cf. Draper and Smith 1981). For each site, the maximum, minimum and mean R_{ref} was computed by applying the respective statistic over all months.

Ecosystem modeling
We used a daily time step ecosystem model that processes the elemental fluxes of carbon, water and nitrogen (Biome-BGC, version 4.1.2, Thornton et al.

2002; Law et al. 2003) to simulate carbon stocks and fluxes for five partici-
pating sites across three biomes. Carbon fluxes had been previously simulated
with this model at all sites except Hesse in France and the Sisters Juniper
(Thornton et al. 2002; Churkina et al. 2003; Law et al. 2003; Turner et al.
2003). Simulated sites included Metolius (old, young), Tharandt, Sisters
Juniper, Harvard, and Hesse representing evergreen needleleaf, woodland/sa-
vanna, mixed deciduous/evergreen and deciduous broadleaf biomes. For the
MXD site, Harvard, we averaged the results from ENF and DBF forest sim-
ulations and took the weighted sum of model output that represented 25 and
75% cover, respectively (Proportions from K. Savage, pers. comm.). Site ini-
tialization variables included soil texture, latitude, longitude and elevation.
Site-specific ecophsyiology (as available) was used to initialize the model for
the ENF, WSV and MXD Metolius, Sisters Juniper and Harvard sites,
respectively (Table 3). General biome ecophysiological parameters were ob-
tained from Churkina et al. (2003), Thornton et al. (2002) and White et al.
(2000) for the ENF Tharandt and DBF Hesse sites.

Long-term (>30 yr) daily surface meteorology was available from Tha-
randt (1952–2000) and Hesse (1970–1999) (G. Churkina, pers comm.). A daily
surface meteorology from 1980 to 1997 were generated for Metolius, Harvard
and Sisters Juniper from the Daymet database (www.daymet.org, Thornton et
al. 2000) to drive the model. Daymet estimates daily minimum, maximum and
average air temperatures, vapor pressure deficit, incoming short wave radia-
tion and day-length from latitude, longitude, elevation and inputs of daily
minimum and maximum temperature and precipitation for the coterminous
US. Gap-filled observations of daily surface meteorology for Harvard was
only available from the AmeriFlux website from 1995 to 1999 and did not
extend into the full suite of measured years of Rs contributed to this analysis.
We therefore used Daymet meteorology for this site. Site-specific adjustments
to the climate database were made for the Metolius and Sisters Juniper sites.
Known effects of a steep precipitation gradient from the Cascade Mountains
to the eastern Metolius sites were corrected for in Law et al. (2001) and used in
this analysis and observed surface meteorology from the flux sites for 1996–
2001 were used to extend the Metolius time series. For the Sisters Juniper site,
local surface meteorology data overlapped and extended beyond Daymet from
1997 to 2002. Observed and simulated temperature from the overlapping years
at the Sisters Juniper and Metolius sites (1997, 1996–1997), which are about
20 km apart, were strongly correlated ($R^2 \geq 0.94$) and the absolute difference
in estimated vs. observed annual precipitation was less than 4.0 mm. We
therefore felt confident that appending existing surface meteorology to Day-
met calculations for these sites would not compromise surface meteorological
drivers generated by Daymet to the Biome-BGC model. Observations of
surface meteorology from the Metolius site included half-hourly temperature,
precipitation, PAR, relative humidity, and VPD. For consistency, we used
MtClim 4.3 (Thornton and Running 1999) to generate short-wave radiation
(W m^{-2}), average daily temperature (°C), vapor pressure difference (Pa) and

Table 3. Site-specific and ecophysiological parameters used in Biome-BGC that varied between sites.

Parameter no.	Units	MEO/MEY[a]	THA	HAR	HES	JUN	Description
1	gN m^{-2} yr^{-1}	0.08	3.2	1.4	1.0	0.08	Current N-deposition
2	yr^{-1}	0.25	0.20	1.00	1.00	0.50	Annual turnover proportion for leaves and roots
3	Dim	2.50	1.40	1.00	1.20	1.40	New fine root C allocation: new leaf C allocation
4	Dim	1	2.2	2.2	1	2.2	New stem C allocation: new leaf C allocation
5	Dim	0.14	0.29	0.23	0.22	0.1	New coarse root C allocation: new stem C allocation
6	kgC kgN^{-1}	50	42	25	20.7	27	C:N of current year's foliage at maturity
7	kgC kgN^{-1}	92	93	55	55	32	C:N of fresh leaf litter, after translocation
8	kgC kgN^{-1}	79	58	48	48	58	C:N of fine roots
9	kgC kgN^{-1}	300	730	550	550	730	C:N of dead wood
10	Prop	0.41	0.24	0.17	0.18	0.25	Leaf litter lignin proportion
11	Prop	0.42	0.22	0.25	0.22	0.42	Fine root lignin proportion
12	m^2 kgC^{-1}	7.7	8.2	32	39.5	12	Canopy average SLA – projected leaf area basis
13	m s^{-1}	0.002	0.006	0.003	0.005	0.006	Maximum stomatal conductance – projected leaf area basis

[a]Ecophysiological characteristics were the same for both MEY and MEO; simulations differed in disturbance histories since time of European settlement.

daylength (s) from the observed site climatologies (THA, HES, JUN, MEO, MEY).

Disturbance history and legacy carbon can have a large effect on soil respiration rates. We used the simulation ensembling and disturbance simulation methods described in Thornton et al. (2002) to isolate disturbance recovery from the variability driven by interannual climate fluctuations. For Harvard, disturbance histories implemented in Biome-BGC were modified to represent biomass removal from harvest and hurricane events based on Foster (1992) and the AmeriFlux website. Disturbance and management included light thinning (4% removal) as a one time harvest ca. 1750. After 1800, 50% removal was implemented in 1850 and 25% removal in 1870 to represent heavy clearing. In 1938, we invoked 20% removal to represent a major hurricane event. At the Hesse site, there was no disturbance prior to 1800. In 1965, a clearcut was followed by thinning (20% removal) in 1999. The Sisters Juniper site was assumed to have no disturbance prior to 1800 as it is an old-growth protected area. In lieu of explicit management records, we assumed fire-suppression with stand-replacing fire in 1800, followed by 50% removal by fire in 1950. Our disturbance regime for Sisters Juniper was based on average reports of fire and demographic histories of western juniper ecosystems (Young and Evans 1981; Miller and Rose 1999). Tharandt is primarily Norway spruce planted ca. 1887 with scant understory development (Churkina et al. 2003; Wang et al. 2003). It is a managed forest with an approximately even age ca. 100 yr. We therefore implemented harvest and subsequent afforestation in 1899 with no disturbance post-1900. We utilized the same disturbance histories and age-class ensembling described in Law et al. (2001) for the Metolius old and young sites. As in Law et al. (2001), the old site was simulated as the average for a dual layer canopy, reflecting the two primary age classes present (50 and 250 yr).

The default model parameterization uses static allocation ratios to relate new growth in fine root and woody tissue to new growth of leaves (Thornton et al. 2002). Simple relationships describing variation of these allocation parameters with stand age were tested in Law et al. (2003) for the Metolius chronosequence. This dynamic allocation was tested for all sites in this analysis and was not robust across the other simulated evergreen needleleaf or deciduous sites (JUN, HAR, THA, HES). As noted in Law et al. (2003), the dynamic allocation changed by ecoregion and biome, so a single allocation pattern with age was not appropriate for all of the sites in this analysis. Therefore, the dynamic allocation logic used in Law et al. (2003) was only implemented for Metolius simulations. All other simulations were with the standard model as described in Thornton et al. (2002).

We included the effects of increasing atmospheric CO_2 from the IS92a data set (Schimel et al. 1994) and N-deposition (NADP 2003). Biome-BGC assumes that N-deposition increases as the anthropogenic CO_2 source increases. This assumption has limitations, but it provides a plausible time sequence of N-deposition when only a historical and a current value are available. Historic

N-deposition rates for all simulations were ca. 1 kg ha^{-1} yr^{-1} for all sites; however, current N-deposition rates ranged from 10 to 32 kg ha^{-1} yr^{-1} at Hesse, Harvard and Tharandt (NADP 2003; D. Lousteau, T. Grünwald, M. Reichstein, pers. comm.). See Table 3 for modeled N-deposition and ecophysiological parameters.

Modeled output was compared to published annual site-level observations of Rs, LAI, and GPP. Output variables included foliar litterfall, NEP, GPP, NPP, Re and its components (soil heterotroph, above and belowground autotrophic respiration), Rs not including coarse and fine woody debris (as measured with chambers), LAI and fine root biomass. All units are gC m^{-2} unless otherwise noted.

All statistical analyses were performed with Sigma Plot 2002 for Windows version 8.02 and S-Plus 6.2 for Windows. All levels of significance reported to $p < 0.05$ unless otherwise noted.

Results and discussion

Average fluxes: day, month and growing season

Daily fluxes

Over all, 31 sites of measured soil respiration (1995–2002), the average flux was 2.1 μmol m^{-2} s^{-1}. The highest daily mean Rs values were from the evergreen needleleafforests Temple and Duke (11.5 and 10.8 μmol m^{-2} s^{-1}), followed by the mixed deciduous/evergreen UMBS (9.9 μmol m^{-2} s^{-1}) site. The lowest measured soil fluxes were during the winter from the MXD Harvard and ENF Howland (ca. 0.05, 0.06 μmol m^{-2} s^{-1}) sites. Of the six sites that measured soil respiration every month of the year (BEP, BEQ, HOW, HAR, UMB and DUK) daily average fluxes ranged from 1.2 to 4.7 μmol m^{-2} s^{-1}. More than 50% of the sites reported maximum daily respiration rates greater than 5.0 μmol m^{-2} s^{-1}, which represents all biomes (DBF, ENF, GRS, MXD and WSV). The sites with the largest and smallest ranges in measured respired fluxes were from the evergreen needleleafforests, Duke and Vielsalm Douglas-fir (10.2 and 1.3 μmol m^{-2} s^{-1}). It is possible that high variability of daily fluxes from Ione grasslands reflect measurements made following rain events and/or over both soil and live leaves, however, removal of this dataset did not significantly influence the average daily fluxes for the GRS biome (data not shown). Additional site-specific summaries and statistics for average fluxes over all data submitted are presented in Appendix 1.

Soil temperature was comparable between forests and non-forested biomes, with highest soil temperatures in GRS (Table 4), where the temperatures ranged over 46 °C. Soil moisture, however, was only comparable between DBF and MXD forested biomes where average soil moisture was relatively high (20–24%) compared with the other sites (15–20%) (Appendix 1). Harvard forest (HAR) had the largest range in observed soil moisture (0.45 m^3 m^{-3}) over the

Table 4. Summary statistics of soil respiration (μmol m^{-2} s^{-1}), soil temperature ($^\circ$ C) and soil moisture (m^3 m^{-3}) across biomes.

Biome	Rs			Soil temperature			Soil moisture		
	n	Mean(SD)[a]	Range	*n*	Mean(SD)	Range	*n*	Mean(SD)	Range
DBF	97	2.4(1.3)*a*	0.4–5.6	97	11(5)*a*	2–20	97	0.18(0.55)*a*	0.10–0.30
ENF	1381	2.4(1.7)*a*	0.1–11.5	1358	12(6)*a*	−3–29	1046	0.16(0.10)*b*	0.03–0.60
GRS	56	2.1(2.3)*b*	0.1–8.2	56	21(10)*b*	−2–44	44	0.23(0.13)*c*	0.09–0.67
MXD	293	3.5(2.2)*c*	0.1–9.9	278	13(5)*a*	0–22	266	0.25(0.11)*a*	0.05–0.47
WSV	327	0.8(0.7)*d*	0.2–4.7	196	22(8)*b*	6–44	186	0.15(0.11)*d*	0.05–0.50

DBF, deciduous broadleaf forest; ENF, evergreen needleleaf forest; GRS, grassland; MXD, mixed deciduous/evergreen forest; WSV, woodland/savanna.
[a]Means (SD) within a column followed by different letters were significantly different ($p < 0.05$).

observation period, and Temple (TML), an evergreen needleleafforest, had the lowest (0.27 m^3 m^{-3}). Data from HAR included an upland plot that was seasonally inundated (flooded), accounting for the large range in soil water content.

Sites with overall strongest relationship between daily mean Rs and soil temperature ($r \geq 0.90$) were all from forested ecosystems and included the ENF and MXD Braschaat de Inslag Forests, Howland, Willow Creek, Vielsalm forests and UMBS. Daily mean Rs was negatively correlated with soil moisture at Vielsalm forests ($r = -0.74$ and -0.78; Douglas-fir and beech sites, respectively). See Appendix 1 for additional details.

Average daily Rs across biomes was 2.3 ± 1.6 (μmol m^{-2} s^{-1}), slightly higher than average daily Rs by site. Average Rs values in a day (μmol m^{-2} s^{-1}) were not significantly different between deciduous and evergreen forest biomes (Table 4). Across biomes, however, the proportion of variance in Rs that was explained by a linear dependence on soil temperature decreased from the mixed deciduous/evergreen and deciduous forests to evergreen and non-forested biomes (Table 5). This was not unexpected, given the

Table 5. Overall contributions of soil temperature and soil moisture to linear relationship of average daily flux (μmol m^{-2} s^{-1}) and root mean square error (RMSE) by biome.

Biome	Soil temperature		Soil moisture	
	R^2	RMSE	R^2	RMSE
DBF	0.65	10.4	0.09[*]	3.80
ENF	0.18	26.17	0.00	3.30
GRS	0.27	8.61	0.00	0.15
WSV	0.01[*]	1.08	0.07	2.73
GRS and WSV	0.06	5.11	0.04[*]	4.45
MXD	0.69	30.50	0.06	9.69
All data	0.05	18.44	0.01	6.47

All relationships were significant ($p < 0.001$) unless otherwise noted. In a stepwise linear regression, soil moisture did not explain any additional variability.
[*]Not significant ($p > 0.1$).

likliehood that moisture variation is more important in water-limited systems such as deserts, grasslands and semiarid woodlands (Reichstein et al. 2002a,b). This may also be partly explained by the lower number of data points in the regression for non-forest biomes and generally lower RMSE (Tables 4 and 5). The linear relationship between Rs and Ts in the mixed deciduous/evergreen forests was strong ($R^2 = 0.69$), and weaker in deciduous broadleaf and evergreen needleleafforests ($R^2 = 0.65$ and 0.18, respectively), and there was no correlation in grassland and woodland/savanna biomes ($R^2 = 0.27$, 0.01). Very low or very high soil moisture has been shown to diminish the temperature response. A multiple, stepwise regression of soil temperature and moisture did not improve estimates of Rs (data not shown). This result is partly expected since soil moisture *per se* does not reflect relative soil water availability between soils with different texture and structure, and Rs is not a linear function of moisture. We did not focus on this effect here, since other studies have already suggested that other indicators of soil water status are more useful, such as relative soil water content, water potential or seasonal distribution of precipitation that may influence patterns of canopy processes and access to deep water storage (e.g., Irvine and Law 2002; Hansen et al. 2002; Reichstein et al. 2003; Xu et al. 2004).

Monthly and growing season fluxes
Biome average Rs during the growing season was lowest in WSV (1.2 ± 0.4) and GRS (1.7 ± 1.1), intermediate in DBF (3.2 ± 0.7) and highest in the MXD and ENF (3.6 ± 1.8; 4.9 ± 1.1) biomes (Figure 2; Table 6). Our average growing season fluxes were strongly differentiated between forested
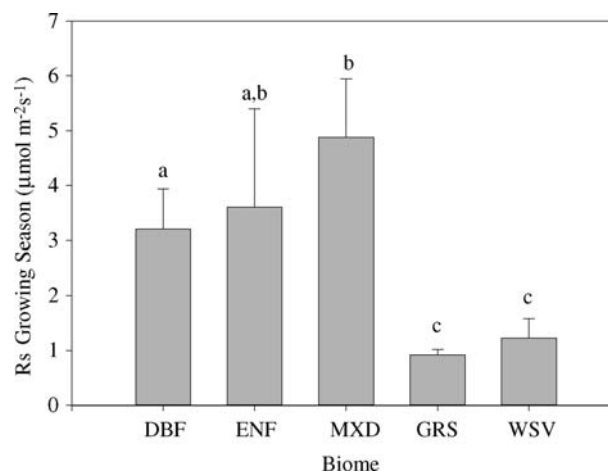

Figure 2. Average and standard deviation of growing season soil respiration for five biomes. Different letters denote significant differences ($p \leq 0.05$) between biomes. Bars represent standard deviation from the mean.

Table 6. Interannual summary statistics by biome of growing season maximum and average soil respiration rates (μmol m^{-2} s^{-1}).

Biome[a]	n(Y)	Maximum Rs		Growing season Rs	
		Mean(SD)[a]	Range	Mean(SD)	Range
DBF	5	3.8(1.4)*a*	2.1–5.6	3.2(0.1)*a*	1.8–3.7
ENF	6	6.0(2.2)*b*	2.2–10.8	3.6(1.8)*a,b*	1.6–8.6
GRS	1	N/A	N/A	1.7(1.1)*c*	0.9–2.9
MXD	7	7.5(1.6)*b*	5.2–9.6	4.9(1.1)*b*	2.2–6.0
WSV	1	N/A	N/A	1.2(0.4)*c*	0.7–1.5

See Methods for growing season criteria. There were not enough data for interannual analyses in GRS and WSV biomes, therefore data were pooled across sites to estimate growing season soil respiration rates. Biome labels as described in Table 4.
[a]Means (SD) within a column followed by different letters were significantly different ($p < 0.05$). N/A, not available.

and non-forested biomes (Figure 2). These results are slightly different from the ranking of seasonal NEP reported in Falge et al. (2002) where relative differences between biomes were not significant (data not shown) suggesting that gross fluxes from aboveground plus woody decomposition may offset belowground contributions to total net fluxes. Aboveground contributions were analyzed in Law et al. (2002) who reported a strong linear relationship between monthly and annual GPP to estimates of evapotranspiration (ET) for forested and grassland ecosystems ($R^2 = 0.58$–0.78). The slope of the relationship between GPP and ET reflects carbon uptake by the canopy relative to the amount of water lost through evaporation and transpiration, or water use efficiency (WUE $=$ GPP/ET). Their ranking of water-use efficiency was almost opposite of our growing season Rs ranking; WUE was highest in evergreen needleleaf forests (4.2 g CO_2/kg H_2O for ENF, 3.4 for GRS, 3.2 for DBF, 3.1 for crops), suggesting the least efficient biomes had the highest Rs. We evaluated the observed maximum and average growing season Rs (μmol m^{-2} s^{-1}) from 11 sites (HAR, HOW, THA, WCR, HES, BEP, BEQ, DUK, MEO, MEY, JUN) as well as previously published estimates of annual Rs (gC m^{-2} yr^{-1}) from 10 sites (HAR, HOW, MEO, MEY, VLD, WDN, WCR, HES, VLB, JUN) relative to annual estimates of GPP (gC m^{-2} yr^{-1}) from eddy flux data (Law et al. 2002). Maximum growing season Rs was weakly correlated with annual GPP ($R^2 = 0.29$; $p < 0.05$) and annual soil respiration or total growing season Rs were not correlated with GPP ($p > 0.1$), although previous studies indicate correlations on shorter time scales within site (e.g., weekly, monthly; e.g., Irvine et al. 2004). We did not have access to weekly or monthly estimates of GPP, nor was it within the scope of this activity to develop summed time-series Rs estimates for each site in this analysis. Concurrent, instantaneous measurements of aboveground contributions (e.g., GPP, photosynthate allocation) with soil respiration that are scaled to weekly and monthly time steps would improve seasonal and phenological quantification of net carbon fluxes.
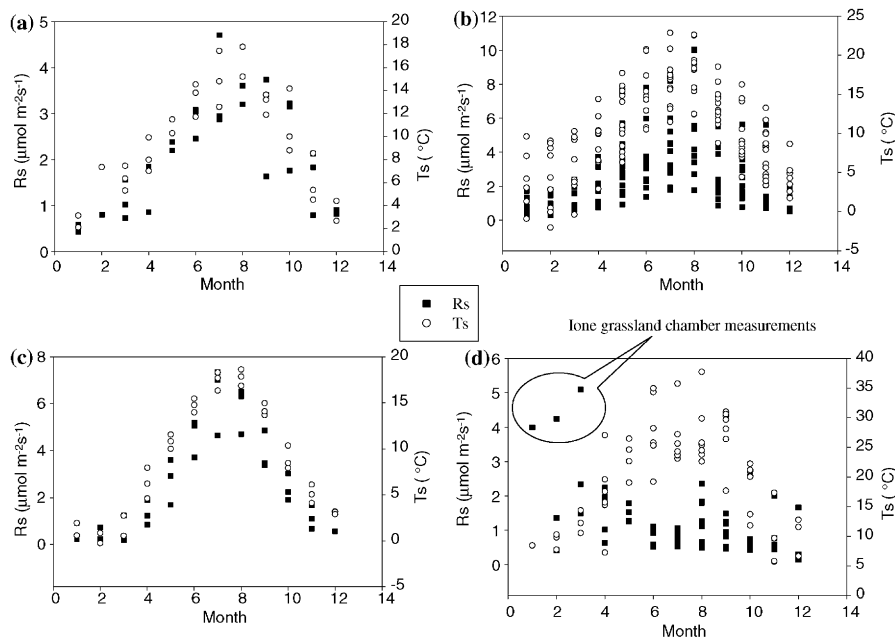
Figure 3. Seasonal changes in measured soil respiration (Rs) and associated soil temperatures (Ts) for: (a) deciduous broadleaf, (b) evergreen needleleaf, (c) mixed deciduous/evergreen, and (d) pooled woodland/savanna and grassland biomes. Monthly average from Ione grassland measurements in Jan, Feb, March reflect ca. 30% contribution of foliar dark respiration in (d). Data represent average measured fluxes in a month.

Seasonal trends averaged over each month in biome-level Rs compared favorably to soil temperature in forested ecosystems when averaged over monthly periods (Figure 3a–c). Interactions between temperature, moisture and biotic factors such as root and foliar allocation likely obscured any temporal relationship between average monthly Rs and soil temperature in woodland/savannas and grasslands (Figure 3d).

The biome-level seasonal amplitude was largest and the duration of 50% of maximum respired fluxes was shortest in grasslands, longer in deciduous broadleaf, and longest in the ENF biome (Figure 3; Table 6). This is consistent with phenology and seasonality of photosynthesis in these biomes. A shorter grassland phenology is likely related to a limited growing season and evergreen needleleafforests are able to assimilate carbon year round as long as climate is favorable ($T_s > 0$ °C). While temporal dynamics of Rs corresponded to soil temperature time series at ENF and DBF sites (Figure 3a, b), at the GRS and WSV sites, lowest respiration rates were observed at the highest temperatures (in summer). This confirms other studies in ecosystems where there is a decline in Rs as the season progresses from the onset of the growing season to summer drought (e.g., Irvine and Law 2002; Curiel Yuste et al. 2003; Xu and Baldocchi

48

2004). Thus, a statistical effect of negative influence of temperature on respiration should not be interpreted as directly suppressive, but can be partially explained by the interaction of soil water availability and temperature influencing soil respiration (e.g., Reichstein et al. 2003). This can appear as hysterisis in correlations between Rs and Ts. In forests, the trend in monthly mean Rs generally reached a maximum in mid-summer, and in GRS and WSV, Rs peaked in spring (Figures 3 and 4a, c, e).

Autotrophic contributions to total Rs associated with growth and maintenance of roots can vary considerably during the growing season (Weinstein et al. 1991; Law et al. 2003). We found that maximum monthly Rs was weakly correlated with maximum LAI and fine root mass ($R^2 = 0.16$, 0.38) and a stepwise regression that includes both variables improved the relationship (multiple $R^2 = 0.56$; Table 7). The contributions of LAI and fine root mass to
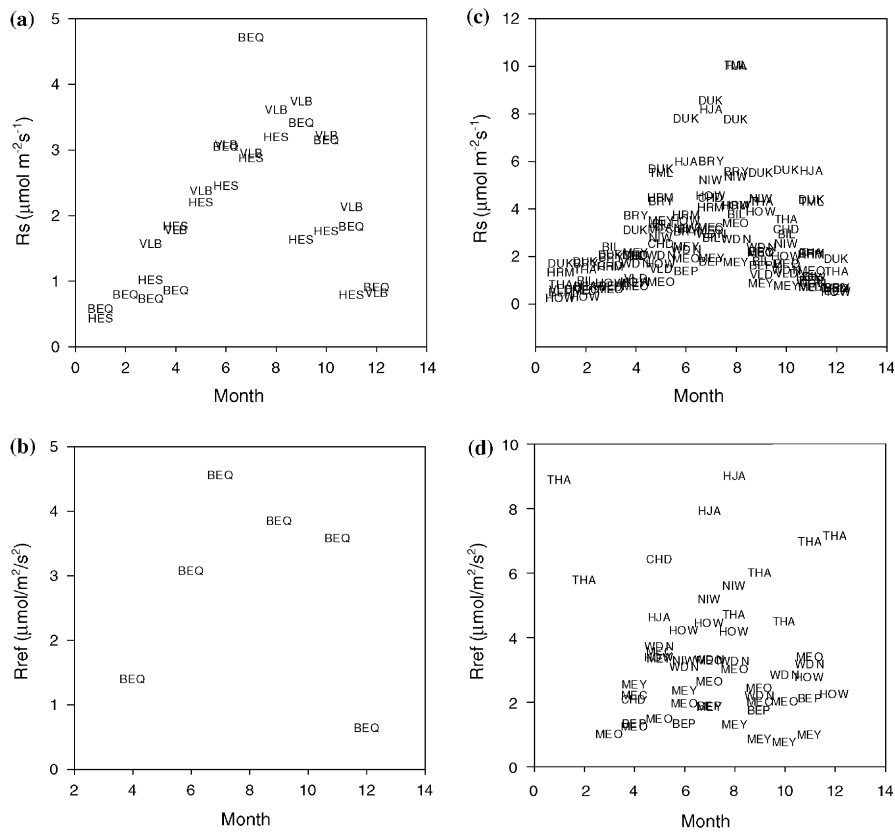

Figure 4. Seasonality of measured (Rs) and standardized soil respiration (R_{ref}) by site for (a,b) deciduous broadleaf (DBF) (c,d) evergreen needleleaf (ENF), (e,f) pooled woodland/savanna and grasslands; and (g,h) mixed deciduous/evergreen forests. Upper panels are Rs and lower panels are R_{ref}.

Figure 4. Continued.

Table 7. Overall contribution of leaf area index (m^{-2} m^{-2}), fine roots (gC m^{-2}) and multiple regression of both variables to maximum and standardized soil fluxes (μmol m^{-2} s^{-1}).

Variable	Maximum Rs		Mean R_{ref}[a]	
	R^2	p	R^2	p
LAI	0.16	< 0.001	0.27	< 0.001
Fine Roots	0.38	0.05	0.40	0.004
Multiple	0.56	0.02	0.68	< 0.001
Stepwise equation	Max Rs $\sim$ 0.70 + 0.08FrootC + 0.48LAI; r^2 = 0.56		Mean R_{ref} $\sim$ 0.24 + 0.007FrootC + 0.38LAI	

Final row indicates model equation of stepwise regression. There were not enough data to do meaningful biome analysis, therefore all data were pooled.
[a] R_{ref} (μmol m^{-2} s^{-1}) is the expected respiration at the reference temperature (T_{ref} = 15 °C).

variability in published values of annual soil respiration (gC m^{-2} yr^{-1}) were stronger than our comparisons with maximum and average growing season fluxes (see text above) (R^2 = 0.48, 0.47; $p \leq$ 0.01; Figure 5a, b), possibly

reflecting integrated seasonal fluctuations in annual estimates that may not be accounted for when determining maximum or growing season estimates.

A multiple regression suggested that both fine root mass and LAI contributed over 65% to annual variability of annual Rs available from the literature (see inset, Figure 5b). Annual estimates of Rs were weakly correlated with both annual foliar litterfall from the current and previous year (R^2 = 0.03, 0.18). A more robust analysis of seasonal fluxes would be to compare monthly estimates of respiration to comparable estimates of fine root carbon and LAI, assuming they represent carbohydrate availability to roots and root respiration where roots account for a large fraction of total Rs. However, if heterotrophic respiration dominates, there is likely to be a lag between litter inputs and decomposition. A full suite of field observations of monthly Rs, LAI, litterfall and fine root mass were not available from all sites, however, greater than 40% of variability in *maximum* Rs was accounted for by the previous years' litterfall at 12 sites, and fine roots contributed only 28% to the variability in maximum Rs (Figure 5c, d). See Table 2 for data contributions by site. A multiple regression using the previous year's litterfall and fine roots improved the relationship (R^2 = 0.56), however, parameter estimates were not significant (p > 0.1), likely because of sparse data on fine roots (data not shown). Our results support other analyses that suggest substrate availability and plant
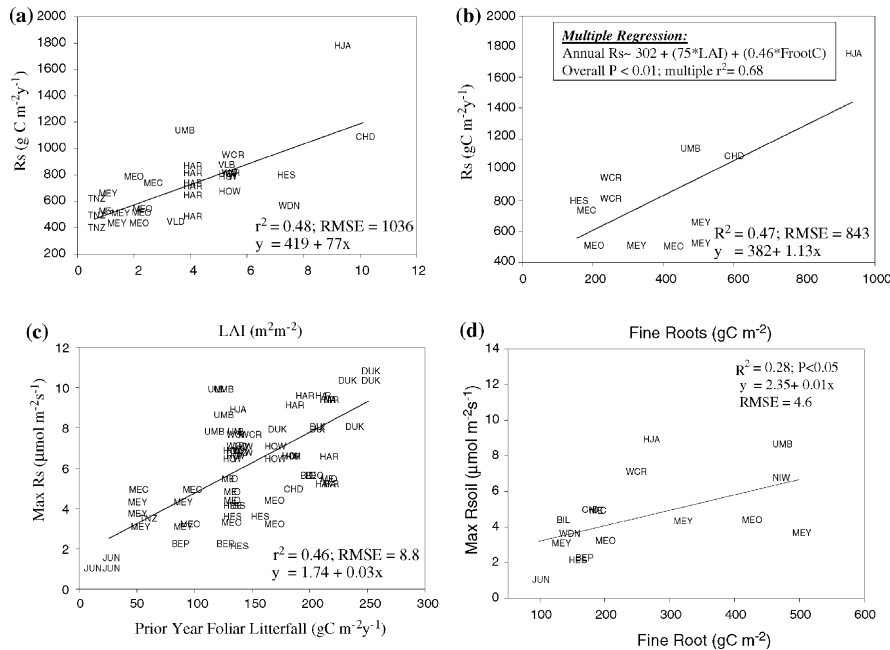

Figure 5. Annual estimates of Rs and (a) leaf area index (LAI), (b) fine root biomass; and maximum measures of Rs to (c) prior year's foliar litterfall; and (c) fine root biomass.

Table 8. Mean (SD) for R_{n15}, R_{ref} and E_a for forests and pooled grassland/shrublands.

Biome	R_{ref} [a]		R_{n15} [b]		E_a [c]
	Mean(SD)	Mean(SD)	Max	Max	Mean(SD)
DBF	2.8(1.4)	3.3(1.1)	6.2	4.6	160(163)
ENF	3.6(2.1)	3.7(1.9)	9.4	9.0	240(428)
MXD	4.3(2.0)	3.8(1.4)	6.2	9.5	171(470)
GRS&WSV	1.8(2.7)	1.3(1.8)	9.1	11.1	104(470)
All biomes	3.4(2.3)	3.1(2.1)	11.1	12.6	197(433)

See text for description of standardized variables. Data are μmol m^{-2} s^{-1}). Biome labels as described in Table 4.

[a] R_{ref} (μmol m^{-2} s^{-1}) is the expected respiration at the reference temperature ($T_{ref} = 15$ °C).
[b] Standardized Rs based on a single T_{ref}.
[c] E_a (°C^{-1}) is a parameter that determines the temperature sensitivity of soil respiration, analogous to the activitation energy from Lloyd and Taylor (1994) Arrenhius equations.

allocation patterns strongly influence soil respiration (e.g., Campbell and Law this issue, Högberg et al. 2001; Janssens et al. 2001; Reichstein et al. 2003; Sanderman et al. 2003; Curiel Yuste et al. 2004; Gu et al. 2004). In general, estimating Rs empirically using simple linear relationships to soil temperature and moisture may be accurate within sites, but do not appear robust at a larger spatial (biome) level.

Standardization models for temperature

To facilitate across-site comparisons of Rs and biological activity, we standardized, or normalized, the observed fluxes for temperature. Base rates of respiration at 15 °C with the general Lloyd and Taylor (1994) parameterization (R_{n15}), and with a month and site-specific re-parameterization (R_{ref}) are reported in Table 8. Site-specific R_{ref} ranged from 0.3 to 9.5 μmol m^{-2} s^{-1} and was highest in the evergreen needleleaf THA forest and lowest in the mixed deciduous/evergreen UMBS forest (Figure 4b, d, f). At WSV and GRS sites, maximum R_{ref} was generally during spring or early summer, reflecting periods of maximum plant growth. The seasonal magnitude of R_{ref} was greatest in the DBF biome and peaked in late summer, reflecting a winter dormant and summer active plant phenology (Figure 4d). Seasonal R_{ref} was not as pronounced in ENF as in the DBF biome, however, R_{ref} in the semi-arid pine sites (MEO, MEY) that experience prolonged periods of soil water deficits showed declines during summer months as reported by Irvine and Law (2002). Our results are consistent with the trends we observed in Rs measurements over the growing season, where seasonal fluxes were substantially greater in deciduous compared to conifer sites. In evergreen needleleaf forests that do not experience late summer drought, Rs rates tend to be highest during mid- to late-summer, possibly related to litter accumulation, and/or root/microbial growth dynamics. Marked seasonality in R_{ref} associated with plant phenological processes
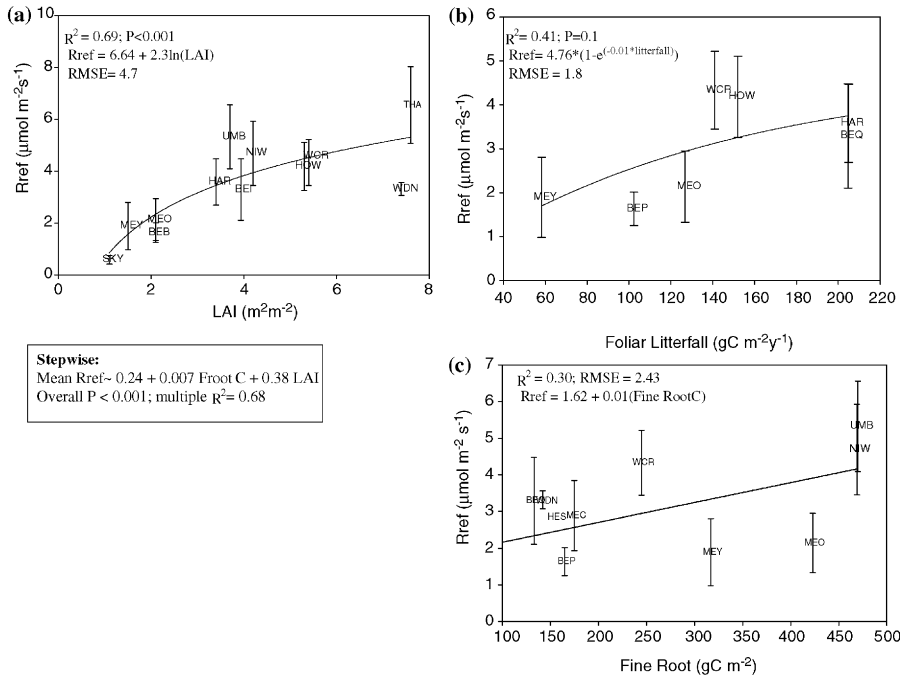
(a)
$R^2 = 0.69; P<0.001$
$Rref = 6.64 + 2.3\ln(LAI)$
$RMSE= 4.7$

Stepwise:
Mean Rref ~ 0.24 + 0.007 Froot C + 0.38 LAI
Overall P < 0.001; multiple R^2= 0.68

(b)
$R^2 = 0.41; P=0.1$
$Rref= 4.76*(1-e^{(-0.01*litterfall)})$
$RMSE= 1.8$

(c)
$R^2 = 0.30; RMSE = 2.43$
$Rref = 1.62 + 0.01(Fine\ RootC)$

Figure 6. Best-fit comparisons of filtered R_{ref} and (a) leaf area index (LAI), (b) mean foliar litterfall; and (c) all R_{ref} and fine root carbon pools. Soil respiration was standardized with site-specific parameters to account for site sensitivity to seasonal temperature. Filtered data were sites that had >2 months R_{ref}, (see Methods text). Stepwise regression was performed on non-filtered data.

support other studies that have suggested linkages between soil respiration and vegetation productivity (Irvine et al. this issue, Sanderman et al. 2003; Curiel Yuste et al. 2004; Gu et al. 2004).

We explored the relationship between standardized R_{ref} and proxies for assimilation and productivity (LAI and fine root mass). Approximately 70% of inter-site variability of our temporally filtered R_{ref} (see Methods text for explanation) was explained by LAI (Figure 6), supporting and extending the relationships reported in Reichstein et al. (2003) where LAI ranged from 1.2 to 4.6. Additionally, the hypothesis that R_{ref} should saturate at high LAI is supported here. LAI is an integrative proxy for plant assimilation and should therefore not be interpreted as a universal mechanistic predictor; however, in a mixed deciduous/evergreen forest, Curiel Yuste et al. (2004) showed that seasonal LAI was strongly correlated with seasonal Rs, suggesting the timing of photosynthetic activity and subsequent belowground allocation respond to seasonal changes in substrate availability. This is also evident from the data, where R_{ref} was markedly different and LAI similar between WDN and THA, possibly related to lower productivity at the cooler, acid rain stressed WDN

Table 9. Linear contribution of GPP, litterfall, fine roots and their relevant combined effects on simulated soil respiration (gC m^{-2} m^{-1}). Biome labels as described in Table 4.

	GPP	Litterfall	Fine roots	Multiple contributions
HAR	0.84	0.05	0.41	0.94; GPP, Fine roots
HES	0.78	0.07	0.45	0.83; GPP, Litterfall
JUN	0.94	0.07	0.04	N/A
MEO	0.96	0.02	0.08	N/A
MEY	0.95	0.07	0.11	N/A
THA	0.78	0.08	0.24	N/A

site (Ulrich 1989) (Figure 6a). Use of seasonal estimates of R_{ref} significantly improved the predictive capability of LAI and fine roots relative to Rs values suggesting that accounting for temperature reduced uncertainties associated with biotic effects on soil respiration (Table 7, Figures 5 and 6). Neither litterfall or fine roots contributed to as much of the variability as accounted for in the filtered R_{ref} and LAI comparisons (Figure 6b, c), and, a stepwise regression with the non-filtered R_{ref} was comparable to R_{ref} calculations that were filtered for sparse data.

Ecosystem modeling and annual fluxes

Process-based ecosystem models estimate components of the carbon cycle, including soil CO_2 efflux but also those mechanisms that contribute to carbon fluxes including allocation and seasonal phenology. Several recent papers have compared ecosystem models to estimates of tower NEE, measurements of NEP and respiration within and among sites (e.g., Law et al. 1999, 2001, 2003; Thornton et al. 2002; Churkina et al. 2003; Kramer et al. 2002). Ecosystem models enable hypothesis testing regarding plant-regulated dynamics (e.g., turnover rates, allocation patterns) and their influence on carbon cycle processes over time frames that extend beyond periods of measurement. In addition, direct influences on carbon fluxes include disturbance history and interannual climate variability as well as indirect influences such as elevated CO_2 and nitrogen deposition, which can be evaluated with process models relative to manipulative and observational experiments. In particular, recent syntheses have highlighted the importance of accounting for disturbance and management histories when estimating net carbon fluxes (Schimel et al. 1997; Law et al. 2002, 2003; Hibbard et al. 2003). We used the ecosystem model, Biome-BGC (Law et al. 2001, 2003; Thornton et al. 2002) to evaluate the influence of management and disturbance on net carbon fluxes for a deciduous broadleaf (HES), mixed deciduous/evergreen (HAR), two evergreen needleleaf (MEO/MEY, THA) and one woodland/savanna (JUN) site. See Table 1 for site label descriptions.
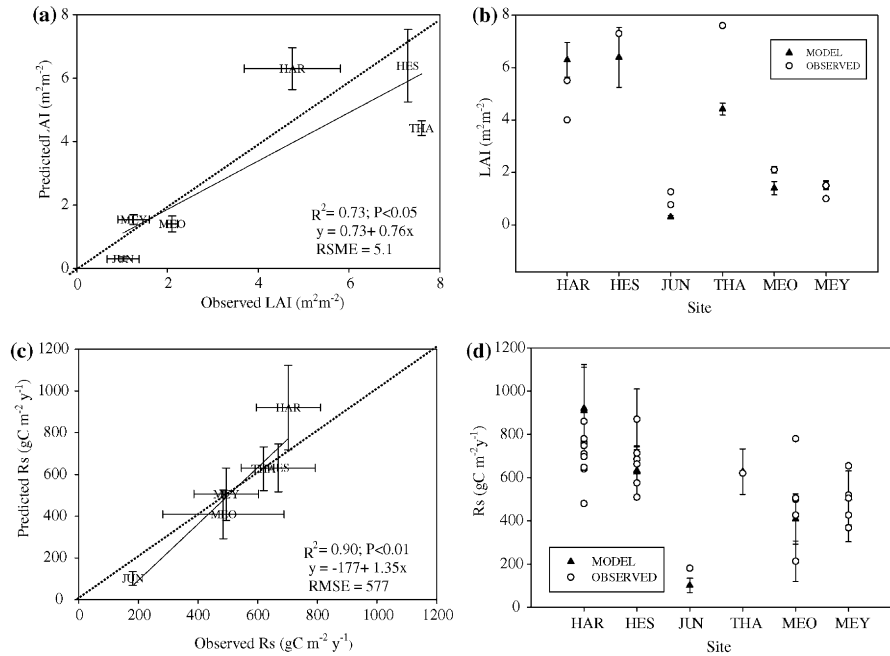
Figure 7. Simulated soil respiration (Rs) for five sites in this synthesis. (See Table 1 for site label definitions). (a) Simulated and observed LAI by site; (b) Relationship of mean simulated LAI to observations; (c) Simulated and observed LAI by site; and (d) relationship of mean simulated Rs to observations. Error bars denote model standard deviation, dotted line represents 1:1 line.

Observed estimates of annual soil respiration and LAI were within one standard deviation of model predictions for the young deciduous and Metolius sites (Figure 7a, b) and interannual variability of annual fluxes reflected in the ensemble simulations suggest that the model is generally within range of observed data (Figure 7c, d). Biome-BGC underestimated LAI in the more mature Sisters Juniper and evergreen sites (Figure 7a). Recall that our modeled response to interannual climate variability is represented by an ensemble of model runs over the number of available years of surface meteorology (see Thornton et al. 2002 for details), however, the representative years for interannual variability were limited by either the available or generated data (see Table 3 and Methods for details). Mean modeled LAI values for all sites were correlated with observations ($R^2 = 0.73$; Figure 7a). Our mean modeled LAI relative to observations for the ENF sites, however, were stronger ($R^2 = 0.88$), comparable to those reported by Thornton et al. (2002) ($R^2 = 0.95$) who simulated ENF sites only. Simulated and observed daily NEP and AET were evaluated by Churkina et al. (2003) for several European forests with Biome-BGC. Their results did not invoke disturbance or management and modeled NEP and AET compared favorably with observations ($R^2 > 0.60$) and their

modeled LAI ranged from 3.2 to 3.6 (m^2 m^{-2}) relative to observed 5.0 (m^2 m^{-2}). Our Tharandt simulations implemented a single clearcut ca.100 ya, and used the same model initialization parameter set and surface meteorology as Churkina et al. (2003). As with Churkina et al. (2003), we implemented current N-deposition rates (see Methods and Table 3), however, our simulated LAI was 4.4 m^2 m^{-2}, suggesting that including disturbance through a single harvest improved LAI predictions relative to observations.

Maximum fine root biomass (gC m^{-2}) simulated by Biome-BGC was generally within range of and correlated with observations ($R^2 = 0.68$; $p < 0.1$; Figure 8a) for all sites except JUN. This may be due to the model assumption of a default belowground carbon allocation for forests that is unrealistic for a semi-arid woodland. Seasonal phenology (or, the amplitude of change within the calendar year) of simulated fine root carbon was strongest in the DBF and MXD sites and, relatively constant for the evergreen Juniper WSV site and weakly seasonal with maximum in late summer for the ENF sites (Figure 8b). This is in contrast to observed phenology with minirhizotrons at the Metolius site, where fine root mass peaks in June (C. Anderson, pers comm.). Both the labile and total simulated litterfall, however, strongly peaked in fall for the DBF and MXD site, with constant inputs for all other sites (Figure 8c; data shown only for total litterfall, labile followed similar patterns).

Other studies that have compared modeled NPP and NEP with observations reported good model agreement when effects of disturbance and/or dynamic carbon allocation with age were considered (e.g., Thornton et al. 2002; Churkina et al. 2003; Law et al. 2003). Accounting for phenology (deciduous vs. evergreen) as well as disturbance histories in this analysis likely contributed to the improved relationship of Biome-BGC estimates of observed pools and fluxes relative to previous studies (e.g., Churkina et al. 2003).

Estimates of GPP from Biome-BGC were strongly correlated with observed annual estimates of soil respiration ($R^2 = 0.84$; Figure 9c). Our modeled ratio of ecosystem respiration (Re):GPP (average = 0.70; range = 0.54–0.89) was comparable to measured values reported by Law et al. (2002) (average = 0.83; range = 0.55–1.2). The trend in the modeled ratio was lower in the DBF site, with higher ratios in the ENF sites (0.54 for Hesse deciduous broadleaf vs. mean 0.73 for evergreen needleleaf), similar to the Law et al. (2002) study, however, the range in Re:GPP was 0.03 in Law et al. (2002) vs. 0.19 in our study. Law et al. (2002) included data from 35 sites including boreal and crop systems not represented in this exercise. The lower ratio in the young Hesse site deciduous broadleaf site could presumably be due to lower cost investments associated with respiring tissue relative to evergreen needleleafforests. Evaluation of carbon use through ratios such as Re:GPP provide insight into the relative contributions of gross to net fluxes. This ratio, however, may underestimate carbon fluxes to the atmosphere in managed forests with short rotations over longer time frames.

Modeled annual Rs was well correlated with published annual estimates of soil respiration ($R^2 = 0.89$; Figure 7c). There were no general patterns of over-
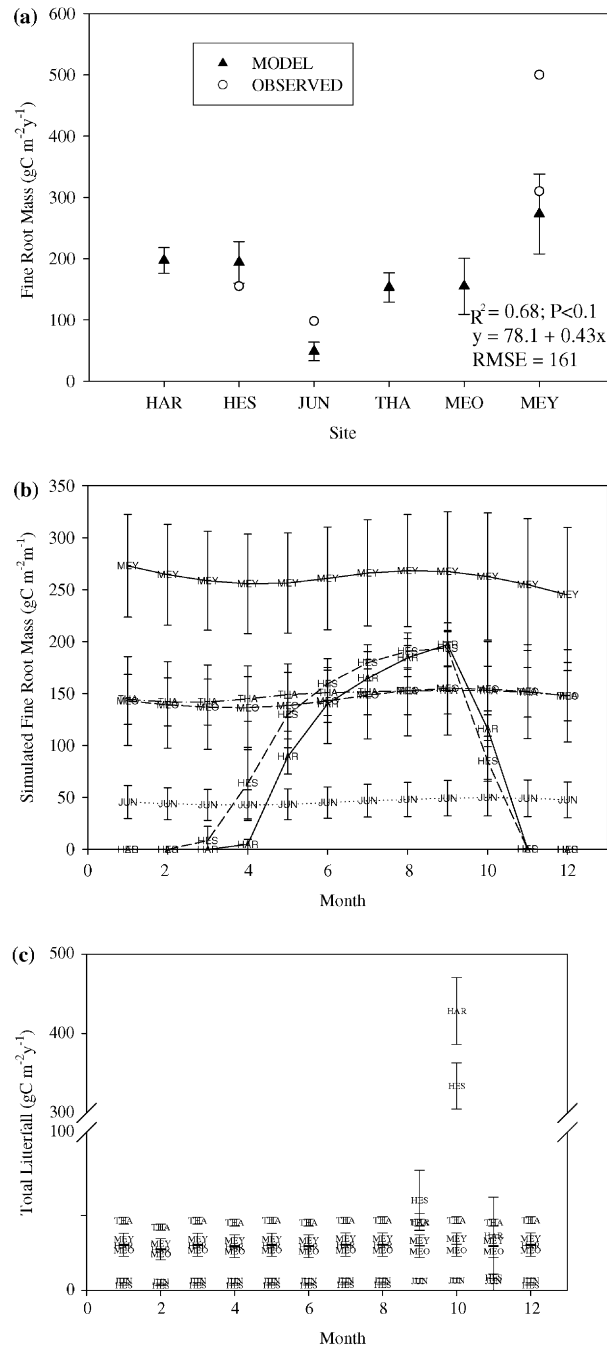
Figure 8. Fine root biomass (gC m^{-2} yr^{-1}) for (a) simulated maximum relative to observed; and (b) simulated monthly for five sites (See Table 1 for site label definitions). Error bars denote modeled standard deviation represented by ensembling approach (see Methods for details).
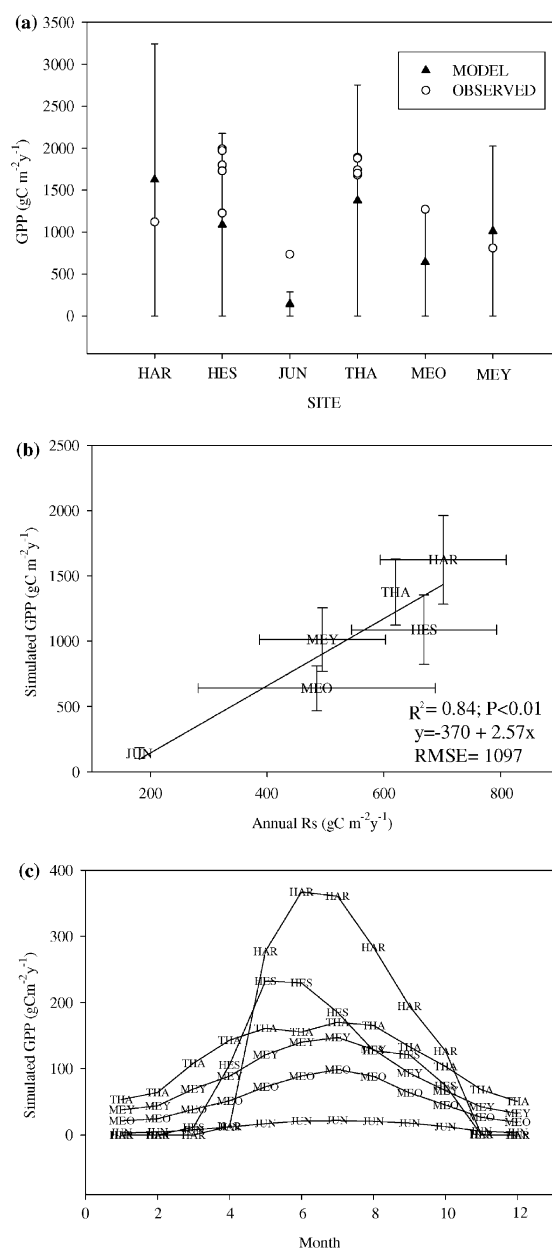
Figure 9. Simulated gross primary production (GPP) for five sites in this synthesis. (a) Simulated and observed GPP by site. Error bars denote modeled standard deviation; (b) Simulated GPP compared to annual estimates of observed Rs. Best fit was linear (solid line); bars represent standard deviation for simulated and observed data (only one estimate of annual Rs was available for JUN and THA); and (c) monthly simulated GPP vs. observed annual Rs for each site. Site labels described in Table 1.

or under-estimation of annual soil respiration fluxes relative to observations across sites (Figure 7a) suggesting that there were no inherent biases in model behavior. Reasonable comparisons between modeled and observed Rs and biological carbon pools, LAI and fine root mass provide a baseline from which to evaluate the relative contributions of simulated root autotrophic (Rroot) and heterotrophic (Rh) components of total Rs.

Correlations of Rs with plant growth may depend on seasonal patterns of assimilated carbon allocated to growth and maintenance of roots and inputs of dead plant material that are not accounted for in annual estimates. Model estimates of monthly Rs were strongly seasonal for the MXD Harvard site, weakly seasonal for the DBF and ENF sites, and constant at the WSV site (Figure 10a), although measurements indicated seasonality of Rs at the Sisters Juniper site (WSV, peak in June was twice that of spring and autumn). Variability of simulated monthly fluxes were strongly controlled by GPP for all sites ($R^2 = 0.78–0.96$; $p < 0.001$) with monthly inputs from fine root carbon and litterfall (multiple $R^2 = 0.94, 0.83$; $p < 0.001$) contributing to the linear effect for the mixed deciduous/evergreen HAR and deciduous broadleaf HES sites, respectively (Table 9). Our simulated results corroborate other studies that have shown multiple factors from above and belowground inputs are important to quantify soil CO_2 efflux, however, the seasonal patterns of carbon inputs are largely unknown in many ecosystems.

Simulated gross carbon fluxes were highest in non-water limited sites (HAR, HES, THA) and decreased sharply with the more semi-arid ENF sites in eastern Oregon (JUN, MEO/MEY) (Figure 9b, c). As was noted for fine root dynamics, the seasonal amplitude in simulated monthly GPP was strongest for the DBF sites and lowest at the Sisters Juniper WSV Figure 9c). Peak GPP was earlier by a month in the warmer deciduous broadleaf, HES relative to the mixed deciduous/evergreen HAR forest (Table 1; Figure 9c). The ENF sites all reached comparable peak periods of GPP in mid-summer. Biome-BGC underestimated Rs, GPP, LAI and fine root carbon for the Sisters Juniper site, possibly for several reasons. First, this site has few interannual observations. The Biome-BGC model had > 20 years of climate data to account for inter-annual variability, however, simulated variability was low relative to observed carbon pools and fluxes. Secondly, we did not simulate an understory in the Juniper site. The dominant understory species is bitterbrush (*Pursia tridenta-ta*), a strong N_2-fixer (Busse et al. 2000). Contributions of inorganic N not accounted for in a juniper-dominated simulation may have contributed to our simulated underestimates of carbon pools and fluxes at this site.

Seasonality of modeled Rs (yearly amplitude = average monthly maximum – minimum) was strongest for the mixed deciduous/evergreen HAR, followed by the young evergreen needleleaf (MEY), then the deciduous broadleaf (HES), evergreen needleleaf THA and MEO, and, finally, the woodland/savanna site, JUN, had the least variable monthly Rs (Figure 10a; Table 10). Seasonality of the modeled autotrophic contribution to total soil respiration varied between sites with the strongest differences in the mixed deciduous/
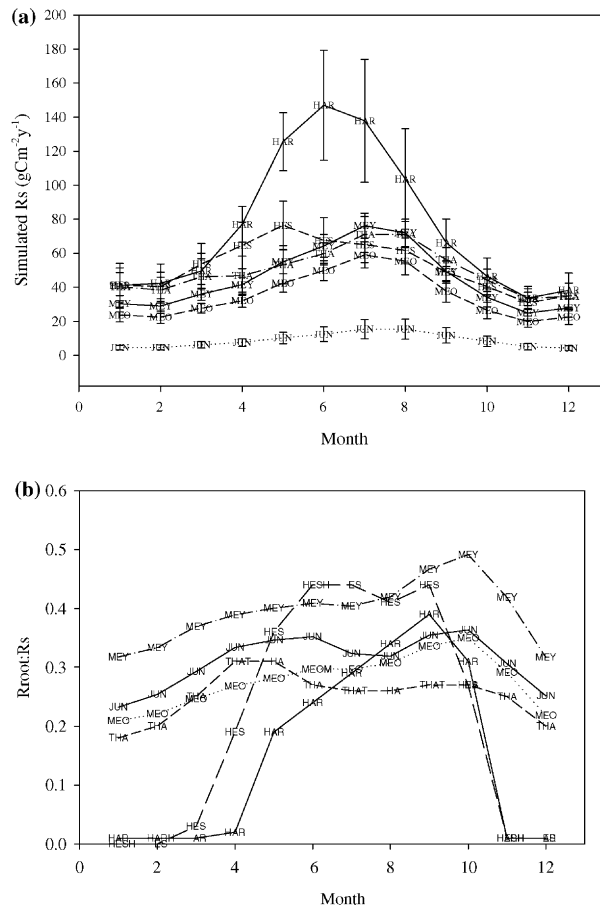
Figure 10. Simulated monthly soil respiration (gC m^{-2} m^{-1}) for five sites representing ENF, DBF and WSV biomes (a) total soil respiration (Rs); and (b) ratio of root respiration (R$_{root}$) to total soil respiration (Rs). Site labels described in Table 1.

evergreen relative to evergreen sites (Table 10). Simulated maximum rates of respired CO$_2$ fluxes in the MXD and DBF sites (Harvard and Hesse) tended to precede those in the ENF and WSV sites by 1–2 months, likely reflecting timing of carbon uptake and carbon allocation to roots (Table 10). The ratio of simulated annual Rroot:Rs was lowest at Harvard (0.20) and highest at the Metolius young site (0.41) (Figure 10; Table 10). Both of the European sites, Hesse and Tharandt, had average Rroot:Rs ratios of 0.25, whereas ratios for the Sisters juniper and Metolius old ponderosa pine sites in eastern Oregon were 0.33 and 0.29. Relative to observations reported in Law et al. (2003), Biome-BGC underestimated the contribution of root autotrophic respiration to Rs for the MEY and MEO sites by 20–42% annually, 23–45% during July and 4–12% in October. Allocation patterns were also consistently elevated in

Table 10. Average annual, amplitude and period of maximum ratio of modeled root respiration:soil respiration (Rroot:Rs). Seasonal amplitude is the maximum Rroot:Rs minus minimum Rroot:Rs. Biome labels as described in Table 4.

	Annual proportion (%)	Seasonal amplitude (gC m^{-2} m^{-1})	Period of maximum Ra:Rs	Period of maximum Rs
HAR	20	114	August/September	June/July
HES	25	45	July/August	May/June
JUN	33	11	June/July	July/August
MEO	29	39	September/October	July/August
MEY	41	51	September/October	July/August
THA	25	39	June/July	July/August

the younger pine site (MEY) during the growing season relative to the mature (MEO) site (Figure 10b). This is consistent with studies that have reported that the proportion of assimilated carbon that is allocated belowground was higher in young than old stands in the water-limited systems (Law et al. 2003). Carbon allocation belowground is also expected to be higher in areas where soil resource availability (N, water) is less favorable (Waring and Running 1998), and Biome-BGC predicted a higher proportion of Rroot to total Rs for nutrient-poor MEY and JUN sites.

Maximum autotrophic contributions tended to lag maximum Rs rates during the growing season by 1–2 months, except at the temperate Tharandt and semiarid Juniper sites where maximum Rs rates preceded and overlapped with maximum Rroot contributions to total fluxes (Table 10). Lagged root autotrophic contributions relative to total maximum fluxes may reflect limited substrate availability and/or environmental conditions that favor heterotrophic activity. In contrast, lagged maximum rates that are co-dominated by heterotrophic and autotrophic contributions may reflect ecosystems that are largely undisturbed, as Tharandt and Juniper were the only simulated sites where management and/or disturbance were not implemented over the last 100 years. The MEO site was simulated as equally co-dominated by old growth (> 250 years) and young (50 years) age stands, and was not 100% undisturbed.

The strong relationships between observed environmental and biotic factors as well as simulated GPP and Rs suggests fast and labile carbon pools dominate respired fluxes over daily and monthly time scales. Do these same controls translate over time and space and provide a basis for understanding the response of carbon storage to environmental change via respiration? What are the indirect effects, such as increasing nitrogen deposition (NDEP) or disturbance on respired fluxes?

We tested the modeled response of NEE, Rs, and soil carbon to historic climate and increased nitrogen deposition and disturbance for the European site, Tharandt where a single harvest occurred ca. 100 years ago and current NDEP rates are greater than 30 kgN ha^{-1} yr^{-1} (T. Grünwald, M. Reichstein pers. comm.). In the undisturbed scenario, NEP follows NDEP closely (Figure 11a), whereas implementation of clearcut in the early 1900s suggests that
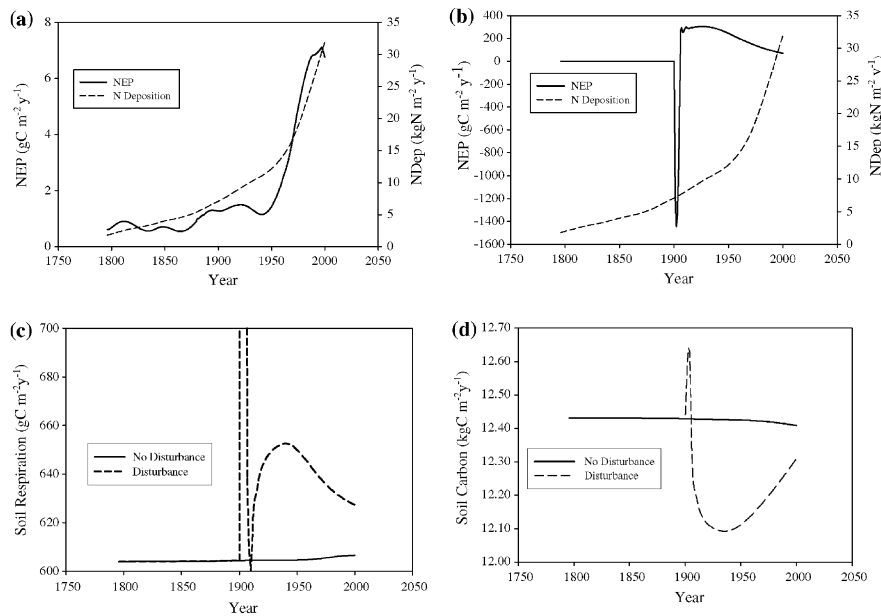
Figure 11. Model sensitivity to disturbance and N-deposition for Tharandt. In undisturbed forests (a) NEP generally follows nitrogen deposition rates, however, clearcutting ca. 100 YA in (b,c) suggest that the managed Tharandt forest is still recovering from clearcut over 100 YA. Current modeled NEP is ca. 70gC m^{-2} yr^{-1}. (d) Modeled trajectory of soil carbon in disturbed and undisturbed Tharandt ENF. Note that simulated NEP (b) returns to comparable levels prior to disturbance, however, Rs and soil carbon (c,d) continue to recover from clearcutting.

NEP and Rs are sharply decoupled from nitrogen inputs and are still recovering from the single disturbance (Figure 11b, c). Similarly, soil carbon shows a similar trend in the disturbed relative to undisturbed simulations (Figure 11d). These kinds of analyses represent the strength of ecosystem modeling, however, we lack the appropriate measures over the longer time scales to evaluate our modeled stocks and fluxes. Clearly, the modeled results suggest that carbon dynamics at Tharandt retain a legacy of disturbance from 100 years ago. While our short-term Rs measurements and extrapolations with temperature and moisture may not provide insight into unique disturbance legacies, they do provide a baseline from which to extrapolate over longer time frames through appropriate representation of site history and disturbances with ecosystem models.

Conclusions

In this analysis, we investigated environmental and biological controls on soil CO$_2$ efflux from a range of northern-hemisphere temperate ecosystems using

empirical regression, Arrhenius standardization for temperature and ecosystem modeling. We have shown that soil temperature is an important factor in predicting soil respiration across a wide range of sites within biomes, however, empirical analyses were not universally robust across sites and biomes. Within sites, including soil moisture improved correlation as expected, but not significantly. Other studies indicated that soil water potential or matric potential were more appropriate indicators of availability of water for biotic activity than soil moisture (Hanson et al. 2000; Irvine and Law 2002). It is clear that soil respiration models that use soil temperature and water to predict soil respiration rates have the potential to work across different sites, but are limited by our understanding about the seasonality of carbon inputs to ecosystems (autotrophic and heterotrophic components).

Accounting for the quality and seasonality of substrate availability from both above and belowground pools and fluxes are important factors in quantifying soil respiration. The timing and availability of carbohydrates for root growth and thus autotrophic respiration are key linkages between soil respiration and net carbon fluxes, such as Rs and GPP. Understanding the balance between autotrophic and heterotrophic contributions to soil respiratory fluxes can be improved by quantifying the processes contributing to soil respiration and for studies that rectify differences in methodological approaches. Our analysis of simulated fluxes suggests that including the seasonal components of plant growth (e.g., GPP), inputs of dead plant material (e.g., litterfall) and root mass are important considerations for quantifying soil respiration. In addition, variable plant allocation, plant age, density, and growth rates are also important and may lead to uncertain and unidentified ecosystem feedbacks (e.g., between photosynthesis and root/mycorrhizal respiration, soil temperature).

Modeled results suggest that increased sampling frequency of belowground root growth and turnover, litterfall and estimates of GPP together with environmental controls can reduce uncertainties of soil CO_2 effluxes. In addition, our modeled results suggest that flux measurements should be made not only in representative terrestrial ecosystems, but in managed and disturbed ecosystems following disturbance events. Our ensembling approach was an indirect comparison to interannual timescales using derived and actual surface meteorology. Actual, long-term climatology do not exist for much of the Earth's surface, however, incorporation of extreme events (e.g., drought, temperature extremes, hurricanes) into interpolated surface meteorology would improve long-term estimates of carbon dynamics to environmental controls.

This study has highlighted the need for additional measurements that reflect plant phenological and microbial response patterns of soil respiration to environmental and disturbance regimes. Site-level process studies have largely focused on temperature and soil moisture response to explain observed soil respiration fluxes, however, these proxies for allocation and heterotrophic dynamics are not sufficient to characterize fluxes at larger spatial and temporal scales. New modeling tools, including data assimilation and parameter optimization, will help identify key constraints and uncertainties in quantifying net

carbon fluxes and pools. These new tools, however, are constrained by available datasets to drive them. Until cooperative syntheses and research activities that cross ecological, international and political borders are made available to the scientific community, these new tools will have limited value. Both the measured and modeled datasets used in this analysis will be made available on the AmeriFlux website (http://public.ornl.gov/ameriflux/) to promote the development of new insights and tools that will become increasingly important to accurately quantify net terrestrial carbon fluxes and their associated uncertainties.

Acknowledgements

Appendix

Appendix 1. Overall summary statistics by site for soil respiration (Rs; μmol m^{-2} s^{-1}), soil temperature (T_s; ° C) and soil moisture (m^{3}m^{-3} * 100) correlation coefficients compare Rs to Ts and soil moisture.

Description	n	Mean	SD	Min	Max	r
Deciduous broadleaf						
Rs	97	2.4	1.3	0.40	5.59	1.00
Ts	97	11.09	4.69	1.45	20.30	0.81
Soil moisture	97	0.20	0.06	0.10	0.30	−0.41
Braschaat_de_Inslag_Oak						
Rs	38	2.30	1.55	0.40	5.59	1.00
Ts	38	10.74	5.05	1.45	18.89	0.90
Soil moisture	38	0.17	0.05	0.10	0.27	−0.67

Appendix 1. Continued

Description	*n*	Mean	SD	Min	Max	*r*
Hesse						
Rs	39	2.39	1.11	0.43	4.40	1.00
Ts	39	12.33	4.20	2.10	20.30	0.75
Soil moisture	NA	NA	NA	NA	NA	NA
Vielsalm (Beech)						
Rs	20	2.60	1.16	0.61	4.63	1.00
Ts	20	9.35	4.34	2.67	15.68	0.87
Soil moisture	20	0.26	0.03	0.20	0.30	−0.74
Evergreen conifer						
Rs	1388	2.42	1.65	1.65	11.48	1.00
Ts	1388	11.50	6.10	−3.00	28.75	0.43
Soil moisture	1388	0.16	0.10	0.03	0.60	0.06
Bilos						
Rs	16	2.55	1.16	0.98	4.34	1.00
Ts	16	14.26	3.74	8.00	20.32	0.82
Soil moisture	NA	NA	NA	NA	NA	NA
Bray						
Rs	22	4.24	1.92	0.69	7.55	1.00
Ts	22	14.46	4.39	3.50	20.11	0.81
Soil moisture	22	0.17	0.11	0.06	0.41	0.09
Duke FACE						
Rs	47	4.70	2.79	0.55	10.79	1.00
Ts	47	15.12	5.70	5.12	24.03	0.89
Soil moisture	47	0.09	0.05	0.03	0.22	0.31
Herm-M						
Rs	24	3.84	2.21	0.65	6.87	1.00
Ts	24	14.10	5.13	5.28	20.10	0.84
Soil moisture	NA	NA	NA	NA	NA	NA
Howland						
Rs	165	2.77	1.66	0.06	6.58	1.00
Ts	165	9.46	5.98	−3.00	21.45	0.92
Soil moisture	165	0.37	0.06	0.26	0.47	0.13
Metolius chronosequence						
Rs	9	2.85	1.32	0.70	4.89	1.00
Ts	9	12.73	5.95	0.00	17.29	0.79
Soil moisture	9	0.14	0.07	0.06	0.28	−0.24
Metolius old site						
Rs	316	2.06	1.09	0.45	5.42	1.00
Ts	316	12.54	5.55	0.25	23.45	0.83
Soil moisture	316	0.11	0.05	0.06	0.23	−0.14
Metolius young site						
Rs	258	1.54	0.91	0.34	4.28	1.00
Ts	258	16.34	5.77	2.83	28.75	0.35
Soil moisture	258	0.10	0.05	0.06	0.25	−0.53
Niwot						
Rs	43	4.51	1.50	2.03	7.44	1.00
Ts	43	12.32	4.89	4.44	8.51	0.14
Soil moisture	43	0.47	0.07	0.38	0.61	−0.61
Oregon Cascade Head						
Rs	12	2.38	0.99	1.03	4.92	1.00
Ts	12	7.81	2.82	3.08	12.32	0.52
Soil moisture	12	0.37	0.04	0.29	0.44	−0.19

Appendix 1. Continued

Description	n	Mean	SD	Min	Max	r
Oregon HJ Andrews						
Rs	11	5.88	2.64	0.77	8.88	1.00
Ts	11	10.45	5.07	0.47	16.89	0.85
Soil moisture	11	0.30	0.08	0.17	0.39	−0.67
Temple						
Rs	4	7.48	3.23	4.30	11.48	1.00
Ts	4	15.95	3.15	11.71	18.67	0.84
Soil moisture	4	0.32	0.03	0.29	0.33	−0.10
Tharandt						
Rs	294	2.60	1.65	0.22	7.80	1.00
Ts	294	6.65	4.32	−0.84	14.31	0.82
Soil moisture	294	0.17	0.06	0.08	0.32	−0.13
Vielsalm (Douglas-fir)						
Rs	15	0.98	0.40	0.41	1.74	1.00
Ts	15	6.42	3.33	0.57	12.06	0.93
Soil moisture	15	0.29	0.01	0.25	0.31	−0.78
Weidenbrunnen						
Rs	127	2.20	0.69	0.47	3.73	1.00
Ts	127	10.20	3.26	1.22	14.99	0.88
Soil moisture	127	0.23	0.06	0.11	0.38	−0.31
Braschaat_de_Inslag_Pine						
Rs	42	1.19	0.48	0.36	2.22	1.00
Ts	42	11.01	4.89	1.42	19.45	0.88
Soil moisture	42	0.17	0.05	0.10	0.27	−0.58
Grassland						
Rs	56	2.15	2.25	0.15	8.16	1.00
Ts	56	20.56	9.51	−2.05	44.16	−0.52
Soil moisture	56	0.23	0.14	0.09	0.67	0.01
Great Basin-Cheatgrass						
Rs	24	1.52	1.50	0.15	5.72	1.00
Ts	24	22.71	9.91	−1.29	44.16	−0.31
Soil moisture	24	0.11	0.05	0.04	0.22	0.25
Great Basin-Crested Wheatgrass						
Rs	21	1.11	0.86	0.27	3.29	1.00
Ts	21	22.33	8.58	−2.05	37.23	−0.34
Soil moisture	21	0.09	0.05	0.04	0.19	0.14
Ione – Measured						
Rs	10	6.02	1.73	2.91	8.16	1.00
Ts	10	10.84	2.30	8.23	15.62	0.41
Soil moisture	10	0.22	0.03	0.17	0.28	0.24
Mixed evergreen/deciduous						
Rs	293	3.52	2.24	0.05	9.88	1.00
Ts	293	12.56	5.27	−0.25	21.80	0.83
Soil moisture	293	0.24	0.11	0.05	0.47	−0.28
UMBS						
Rs	79	4.56	2.39	0.70	9.88	1.00
Ts	79	12.64	5.82	−0.25	21.34	0.93
Soil moisture	79	0.13	0.50	0.50	0.23	−0.49
Willow creek						
Rs	18	3.90	2.16	0.56	7.62	1.00
Ts	18	12.65	5.22	2.89	19.68	0.90

Appendix 1. Continued

Description	*n*	Mean	SD	Min	Max	*r*
Soil moisture	18	0.24	0.10	0.05	0.39	0.18
Harvard						
Rs	197	3.06	2.04	0.05	8.59	1.00
Ts	197	12.40	5.14	0.52	21.79	0.82
Soil moisture	197	0.30	0.09	0.07	0.47	0.02
Woodland/savanna						
Rs	195	0.89	0.77	0.15	4.66	1.00
Ts	195	20.28	8.77	3.00	43.79	−0.10
Soil moisture	195	0.16	0.11	0.05	0.50	0.25
Great Basin – Juniper						
Rs	19	1.45	1.08	0.25	4.66	1.00
Ts	19	22.12	5.96	10.55	31.30	−0.19
Soil moisture	19	0.09	0.05	0.04	0.18	0.00
Great Basin – Sage						
Rs	20	1.08	0.81	0.25	2.96	1.00
Ts	20	24.59	8.15	9.34	43.79	−0.40
Soil moisture	20	0.07	0.05	0.03	0.19	−0.12
Great Basin – (All)						
Rs	84	1.30	1.12	0.15	5.72	1.00
Ts	84	22.93	8.29	−2.05	44.16	0.25
Soil moisture	84	0.09	0.05	0.03	0.22	−0.37
Oregon-Juniper/Sage						
Rs	87	0.57	0.31	0.18	1.51	1.00
Ts	87	20.81	6.51	6.93	32.62	0.42
Soil moisture	87	0.09	0.02	0.05	0.16	0.22
Sky Oaks young						
Rs	11	0.59	0.20	0.30	0.92	1.00
Ts	11	22.53	9.43	6.66	34.05	0.39
Soil moisture	11	0.21	0.04	0.16	0.30	−0.08
Sky Oaks old						
Rs	4	0.70	0.07	0.62	0.79	1.00
Ts	4	28.98	4.98	22.69	33.12	0.70
Soil moisture	4	0.26	0.03	0.23	0.30	0.58
Sky_Oaks (All)						
Rs	15	0.62	0.18	0.30	0.92	1.00
Ts	15	24.25	8.81	6.66	34.05	0.43
Soil moisture	15	0.20	0.04	0.16	0.30	−0.14
Tonzi						
Rs	23	1.13	0.82	0.38	3.47	1.00
Ts	23	26.05	10.51	9.84	42.33	−0.63
Soil moisture	23	0.13	0.10	0.05	0.37	0.67

NA = not available.

References

Borken W., Xu Y-J., Davidson E.A. and Beese F. 2002. Site and temporal variation of soil respiration in European beech, Norway spruce, and Scots pine forests. Global Change Biol. 8: 1205–1216.

Bowling D.R., McDowell N., Bond B., Law B.E. and Ehrlinger J. 2002. ^{13}C content of ecosystem respiration is linked to precipitation and vapor pressure deficit. Oecologia 131: 113–124.

Busse M.D. 2000. Suitability and use of the ^{15}N-isotope dilution method to estimate nitrogen fixation by actinorhizal shrubs. Forest Ecol. Manage. 136: 85–95.

Butnor J.R., Johnsen K.H., Oren R. and Katul G.G. 2003. Reduction of forest floor respiration by fertilization on both carbon dioxide-enriched and reference 17-year-old loblolly pine stands. Global Change Biol. 9: 849–861.

Campbell J. and Law B.E. 2004. Forest soil respiration across three climatically-distinct chrono-sequences in Oregon. Biogeochemistry this issue.

Churkina G., Tenhunen J., Thornton P., Falge E.M., Elbers J.A., Erhard M., Grünwald T., Kowalski A.S., Rannik U. and Sprinz D. 2003. Analyzing the ecosystem carbon dynamics of four European coniferous forests using a biogeochemistry model. Ecosystems 6: 168–184.

Compton J.E. and Boone R.D. 2000. Long-term impacts of agriculture on soil carbon and nitrogen in New England forests. Ecology 81(8): 2314–2330.

Curiel Yuste J., Janssens I.A., Carrara A. and Ceulemans R. 2004. Annual Q_{10} of soil respiration reflects plant phenological patterns as well as temperature sensitivity. Global Change Biol. 10: 161–169.

Curiel Yuste J., Janssens I.A., Carrara A., Meiresonne L. and Ceulemans R. 2003. Interactive effect of temperature and precipitation on soil respiration in a temperate maritime pine forest. Tree Physiol. 23: 1263–1270.

Curtis P.S., Hanson P.J., Bolstad P., Barford C., Randolph J.C., Schmid H.P. and Wilson K.B. 2002. Biometric and eddy-covariance based estimates of annual carbon storage in five eastern North American deciduous forests. Agricult. Forest Meteorol. 113: 3–19.

Davidson E.A., Belk E. and Boone R.D. 1998. Soil water content and temperature as independent of confounded factors controlling soil respiration in a temperate mixed hardwood forest. Global Change Biol. 4: 217–227.

Davidson E.A., Savage K., Bolstad P., Clark D.A., Curtis P.S., Ellsworth D.S., Hanson P.J., Law B.E., Luo Y., Pregitzer K.S., Randolph J.C. and Zak D. 2002. Belowground carbon allocation in forests estimated from litterfall and IRGA-based soil respiration measurements. Agricult. Forest Meteorol. 113: 39–51.

Draper N. and Smith H. 1981. Appl. Regres. Anal.. John Wiley, New York.

Falge E., Baldocchi D., Tenhunen J., Aubinet M., Bakwin P., Bergigier P., Bernhover C., Burba G., Clement R., Davis K.J., Elbers J.A., Goldstein A.H., Grelle A., Granier A., Gudmundsson J., Hollinger D., Kowalski A.S., Katul G., Law B.E., Malhi Y., Meyers T., Monson R.K., Munger J.W., Oechel W., Paw U., K.T., , Pilegaard K., Rannik U., Rebmann C., Suyker A., Valentini R., Wilson D. and Wofsy S. 2002. Seasonality of ecosystem respiration and gross primary production as derived from FLUXNET measurements. Agricult. Forest Meteorol. 113: 53–74.

Foster D.R. 1992. Land-use history (1730–1990) and vegetation dynamics in central New England, USA. J. Ecol. 80: 753–771.

Finzi A.C. and Schlesinger W.H. 2003. Soil–nitrogen cycling in a pine forest exposed to 5 years of elevated carbon dioxide. Ecosystems 6: 444–456.

Gaudinski J.B., Trumbore S.E., Davidson E.A. and Zheng S. 2000. Soil carbon cycling in a temperate forest: radiocarbon-based estimates of residence times, sequestration rates and partitioning of fluxes. Biogeochemistry 51: 33–69.

Grünwald Th. 2002. Langfristige Beobachtungen von Kohlendioxidflüssen mittels Eddy-Kovari-anz-Technik über einem Altfichtenbestand im Tharandter Wald. Ph.D. Thesis, Technical University Dresden, Dresden, Germany, pp. 148.

Gu L., Post W.M. and King A.W. 2004. Fast labile carbon turnover obscures sensitivity of heterotrophic respiration from soil to temperature: A model analysis. Global Biogeochem. Cycles 18: GB1022.

Hanson P.J., Edwards N.T., Garten C.T. and Andrews J.A. 2000. Separating root and soil microbial contributions to soil respiration: A review of methods and observations. Biogeochemistry 48: 115–146.

68

Hibbard K.A., Schimel D.S., Archer S., Ojima D.S. and Parton W. 2003. Grassland to woodland transitions: Integrating changes in landscape structure and biogeochemistry. Ecological Appl. 13(4): 911–926.

Högberg P., Nordgren A., Buchmann N., Taylor A.F.S., Ekblad A., Högberg M.N., Nyberg G., Ottosson-Lofvenius M. and Read D.J. 2001. Large-scale forest girdling shows that current photosynthesis drives soil respiration. Nature 411(6839): 789–792.

IPCC. 2001. Summary for Policymakers: WG I "Climate Change 2001: The Scientific Basis". Intergovernmental Panel on Climate Change.

Irvine J. and Law B.E. 2002. Seasonal soil CO_2 effluxes in young and old ponderosa pine forests. Global Change Biol. 8: 1183–1194.

Irvine J., Law B.E. and Kurpius M. 2004. Coupling of canopy gas exchange with root and rhizosphere respiration in ponderosa pine: correlations or controls? Biogeochemistry this issue.

Janssens I.A., Lankreijer H., Matteucci G., Kowalski A.S., Buchmann N., Epron D., Pilegaard K., Kutsch W., Longdoz B., Grunwald T., Montagnani L., Dore S., Rebmann C., Moors E.J., Grelle A., Rannik U., Morgenstern K., Oltchev S., Clement R., Gudmundsson J., Minerbi S., Berbigier P., Ibrom A., Moncrieff J., Aubinet M., Bernhofer C., Jensen N.O., Vesala T., Granier A., Schulze E.D., Lindroth A., Dolman A.J., Jarvis P.G., Ceulemans R. and Valentini R. 2001. Productivity overshadows temperature in determining soil and ecosystem respiration across European forests. Global Change Biol. 7(3): 269–278.

Kramer K., Leinonen I., Bartelink H.H., Berbigier P., Borghetti M., Bernhofer C., Cienciala E., Dolman A.J., Froer O., Gracia C.A., Granier A., Grünwald T., Hari P., Jans W., Kellomaki S., Loustau D., Magnani F., Markkanen T., Matteucci G., Mohren G.M.J., Moors E., Nissinen A., Peltola H., Sabate S., Sanchez A., Sontag M., Valentini R. and Vesala T. 2002. Evaluation of six process-based forest growth models using eddy-covariance measurements of CO_2 and H_2O fluxes at six forest sites in Europe. Global Change Biol. 8: 213–230.

Law B.E., Falge E., Gu L., Baldocchi D.D., Bakwin P., Berbigier P., Davis K., Dolman A.J., Falk M., Fuentes J.D., Goldstein A., Granier A., Grelle A., Hollinger D., Janssens I.A., Jarvis P., Jensen N.O., Katul G., Mahli Y., Matteucci G., Meyers T., Monson R., Munger W., Oechel W., Olson R., Pilegaard K., Paw K.T., Thorgeirsson H., Valentini R., Verma S., Vesala T., Wilson K. and Wofsy S. 2002. Environmental controls over carbon dioxide and water vapor exchange of terrestrial vegetation. Agricult. Forest Meteorol. 113: 97–120.

Law B.E., Ryan M.G. and Anthoni P.M. 1999. Seasonal and annual respiration of a ponderosa pine ecosystem. Global Change Biol. 5(2): 169–182.

Law B.E., Sun O., Campbell J., Van Tuyl S. and Thornton P. 2003. Changes in carbon storage and fluxes in a chronosequence of ponderosa pine. Global Change Biol. 9: 510–524.

Law B.E., Thornton P.E., Irvine J., Anthoni P.M. and Van Tuyl S. 2001. Carbon storage and fluxes in ponderosa pine forests at different development stages. Global Change Biol. 7(7): 755–777.

Lloyd J. and Taylor J.A. 1994. On the temperature dependence of soil respiration. Funct. Ecol. 8: 315–323.

Longdoz B., Yernaux M. and Aubinet M. 2000. Soil CO_2 efflux measurements in a mixed forest: impact of chamber disturbances, spatial variability and seasonal evolution. Global Change Biol. 6: 907–917.

Miller R.F. and Rose J.A. 1999. Fire history and western juniper encroachment in a sagegrush steppe. J. Range Manage. 52: 550–559.

National Atmospheric Deposition Program (NADP). 2003. National Atmospheric Deposition Program 2002 Annual Summary. NADP Data Report 2003–01. Illinois State Water Survey, Champaign, IL.

Raich J.W. and Schlesinger W.H. 1992. The global carbon dioxide flux in soil respiration and its relationship to vegetation and climate. Tellus. Ser. B. 44: 81–99.

Raich J.W. and Potter C.S. 1995. Global patterns of carbon dioxide emissions from soils. Global Biogeochem. Cycles 9: 23–36.

Raich J.W., Potter C.S. and Bhagwati D. 2002. Interannual variability in global soil respiration, 1980–1994. Global Change Biol. 8: 800–812.

Rebmann C., Anthoni P., Falge E., Göckede M., Mangold A., Subke J.A., Thomas C., Wichura B., Schulze E.D., Tenhunen J.D. and Foken T. 2004. Carbon budget of a spruce forest ecosystem. In: Matzner (ed.), Biogeochemistry of Forets Catchments in a Changing Environment. Ecological Studies Vol. 172. Springer, Heidelberg, Germany.

Reichstein M., Rey A., Freibauer A., Tenhunen J., Valentini R., Banza J., Casals P., Cheng Y.F., Grunzweig J.M., Irvine J., Joffre R., Law B.E., Loustau D., Miglietta F., Oechel W., Ourcival J.M., Pereira J.S., Peressotti A., Ponti F., Qi Y., Rambal S., Rayment M., Romanya J., Rossi F., Tedeschi V., Tirone G., Xu M. and Yakir D. 2003. Modeling temporal and large-scale spatial variability of soil respiration from soil water availability, temperature and vegetation productivity indices. Global Biogeochem. Cycles 17(4): Art. No. 1104.

Reichstein M., Tenhunen J.D., Ourcival J.M., Rambal S., Dore S. and Valentini R. 2002a. Ecosystem respiration in two mediterranean evergreen holm oak forests: drought effects and decomposition dynamics. Funct. Ecol. 16: 27–39.

Reichstein M., Tenhunen J.D., Roupsard O., Ourcival J.-M., Rambal S., Miglietta F., Peressotti A., Pecchiari M., Tirone G. and Valentini R. 2002b. Severe drought effects on ecosystem CO_2 and H_2O fluxes in three mediterranean evergreen ecosystems: revision of current hypotheses? Global Change Biol. 8: 999–1017.

Sanderman J., Amundson R.G. and Baldocchi D.D. 2003. Application of eddy covariance measurements to the temperature dependence of soil organic matter mean residence time. Global Biogeochem. Cycles 17: No. 2, 1061, doi:10.1029/2001GB001833.

Savage K.E. and Davidson E.A. 2001. Interannual variation of soil respiration in two New England forests. Global Biogeochem. Cycles 15(2): 337–350.

Schimel D.S., Alves D., Enting I., Heimann M., Joos F., Raynaud D. and Wigley T. 1996. Radiative Forcing of Climate Change in Climate Change: The Science of Climate Change. In: Houghton J.T. et al. (ed.), Cambridge University Press, New York pp.1–40.

Schimel D.S., Emanual W., Rizzo B. and VEMAP participants 1997. Continental scale variability in ecosystem processes – models, data, and the role of disturbance. Ecological Monographs 67: 251–271.

Schlesinger W.H. 1990. Evidence from chronosequence studies for a low carbon-storage potential of soils. Nature 348: 232–234.

Scott-Denton L.E., Sparks L.L. and Monson R.K. 2003. Spatial and temporal controls of soil respiration rate in a high-elevation, subalpine forest. Soil Biol. Biochem. 35: 525–534.

Subke J.A., Buchmann N. and Tenhunen J.D. 2004. Soil CO_2 fluxes in Spruce forests – temporal and spatial variation, and environmental controls. In: Matzner (ed.), Biogeochemistry of Forest Catchments in a Changing Environment. Ecological Studies vol. 172. Springer, Heidelberg, Germany.

Subke J.-A., Reichstein M. and Tenhunen J.D. 2003. Explaining temporal variation in soil CO_2 efflux in a mature spruce forest in Southern Germany. Soil Biology & Biochemistry 35: 146–1483.

Thornton P.E., Law B.E., Gholz H.L., Clark K.L, Falge E., Ellsworth D.S., Goldstein A.H., Monson R.K., Hollinger D., Falk M., Chen J. and Sparks J.P. 2002. Modeling and measuring the effects of disturbance history and climate on carbon and water budgets in evergreen needleleaf forests. Agricult. Forest Meteorol. 113: 185–222.

Thornton P.E. and Running S.W. 1999. An improved algorithm for estimating incident daily solar radiation from measurements of temperature, humidity, and precipitation. Agricult. Forest Meteorol. 93: 211–228.

Turner D.P., Ritts W.D., Cohen W.B., Gower S.T., Zhao M., Running S.W., Wofsy S.C., Urbanski S., Dunn A. and Munger J.W. 2003. Scaling gross primary production (GPP) over boreal and deciduous forest landscapes in support of MODIS GPP product validation. Remote Sensing Environ. 88: 256–270.

Ulrich B. 1989. Effects of acidic precipitation on forest ecosystems in Europe. In: Adriano D.C. and Johnson A.H. (eds), Acidic Precipitation. Vol. 2. Springer-Verlag, Berlin, pp. 189–272.

Valentini R., Matteucci G., Dolman A.J., Schulze E.D., Rebmann C., Moors E.J., Granier A., Gross P., Jensen N.O., Pilegaard K., Lindroth A., Grelle A., Bernhofer C., Grünwald T.,

Aubinet M., Ceulemans R., Kowalski A.S., Vesala T., Rannik U., Berbigier P., Loustau D., Guomundsson J., Thorgeirsson H., Ibrom A., Morgenstern K., Clement R., Moncrieff J., Montagnani L., Minerbi S. and Jarvis P.G. 2000. Respiration as the main determinant of carbon balance in European forests. Nature 404(6780): 861–865.

Wang Q., Tenhunen J., Falge E., Bernhover C., Granier A. and Vesala T. 2003. Simulation and scaling of temporal variation in gross primary production for coniferous and deciduous temperate forests. Global Change Biol. 10: 37–51.

Waring R. and Running S.S. 1998. Forest Ecosystems: Analysis at Multiple Scales. 2nd ed. Academic Press, New York.

Weinstein D.A., Beloin R.M. and yanai R.D. 1991. Modeling changes in red spruce carbon balance and allocation in response to interacting ozone and nutrient stresses. Tree Physiol. 9: 127–146.

White M.A., Thornton P.E., Running S.W. and Nemani R.R. 2000. Parameterization and sensitivity analysis of the Biome-BGC terrestrial ecosystem model: net primary production controls. Earth Inter. 4(3): 1–85.

Xu L. and Baldocchi D.D. 2004. Seasonal variation in carbon dioxide exchange over a Mediterranean annual grassland in California. Agricult. Forest Meteorol. 123: 79–96.

Xu L., Baldocchi D.D. and Tang J. 2004. How soil moisture, rain pulses and growth alter the response of ecosystem respiration to temperature. Global Biogeochem. Cycles 18: GB4002, doi:10.1029/2004GB002281.

Young J.A. and Evans R.A. 1981. Demography and fire history of a western juniper stand. J. Range Manage. 34(6): 501–506.